AD-A174 105 XCP (EXPENDABLE CURRENT PROFILER) PERFORMANCE NEAR THE GEOMAGNETIC EQUATOR(U) WASHINGTON UNIV SEATTLE APPLIED PHYSICS LAB M A KENNELLY ET AL JUL 86 APL-UW-8607 1/1

UNCLASSIFIED N00014-82-C-0038 F/G 20/4 NL

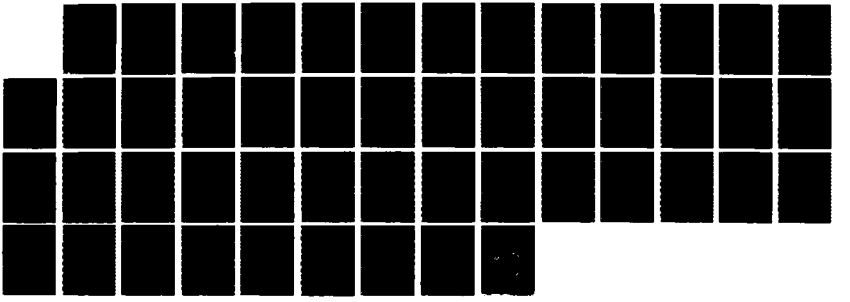

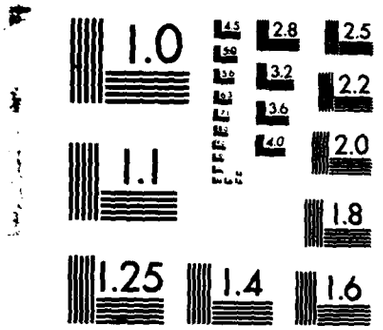

XCP Performance Near the Geomagnetic Equator

APL-UW 8607
July 1986

Contract N000-14-82-C-0038

Approved for public release.

XCP Performance Near the Geomagnetic Equator

by
M. A. Kennelly
P. A. McKeown
T. B. Sanford

APL-UW 8607
July 1986

Applied Physics Laboratory University of Washington
Seattle, Washington 98105

Contract N000-14-82-C-0038

Approved for public release.

ABSTRACT

Velocity profiles collected with an expendable current profiler (XCP) and with a recoverable free-fall profiler, TOPS (Total Ocean Profiling System), are compared in the vicinity of the geographic and geomagnetic equators. The XCP operates on the principles of motional induction, measuring the electric currents that result from the movement of seawater through the vertical component of the earth's magnetic field. Induced electric currents are interpreted in terms of the oceanic velocity structure. TOPS is a freely falling profiler that utilizes acoustic tracking techniques to measure velocity structure at the longer vertical wavelengths ($\lambda > 20$ m) and an onboard two-axis acoustic velocimeter to measure finestructure (20 m $> \lambda >$ 20 cm). Previous mid-latitude intercomparisons showed these two profilers to agree within 1-2 cm/s rms. The present study, conducted in March-April 1982, took place in the eastern equatorial Pacific to compare profiler performance near the magnetic equator (8°10'S at 95°W). Results of measurements made along a transect from 3°N to 8°S are presented. As the magnetic equator is approached, the performance of the XCP relative to that of TOPS degrades because the vertical component of the geomagnetic field diminishes. The XCP performs usefully (noise < 10 cm s^{-1}) to within 1.5° of the magnetic equator for the east component of velocity. This corresponds to $F_z/F_h = 0.05$, where F_z/F_h is the ratio of the vertical component of the earth's magnetic field to the horizontal component. Measurements were also acquired along the equator west of 95°W. The two major sources of error seem to be inadequate compensation for the fall rate and vessel interference. Probe-to-probe variability is attributed to electronic phase differences, which are more noticeable near the magnetic equator.

TABLE OF CONTENTS

LIST OF FIGURES

LIST OF TABLES

1. INTRODUCTION

To observe small-scale variability in the eastern equatorial Pacific, profiles of velocity and temperature were acquired using 37 expendable current profilers (XCPs). These measurements were made aboard the NOAA vessel *Discoverer* from 24 March to 27 April 1982 during a cruise of the Equatorial Pacific Ocean Climate Studies (EPOCS) Program. Measurements were made along 95°W from 3°N to 8°S and along the equator west of 95°W.

EPOCS is a NOAA sponsored research program that commenced in 1979 with the goal of understanding the mechanisms of climate variations associated with air-sea interactions in the equatorial Pacific Ocean. The objective of the March-April cruise was to continue the observation program, with intensive sampling on a north-south transect across the equator at 95°W.

The objectives of the XCP operations on this cruise were as follows: to compare the velocity profiles obtained using the XCP with those acquired from TOPS (Total Ocean Profiling System, which is NOAA/PMEL's free-fall velocity profiler), as in Sanford (1982); to study the feasibility of utilizing XCPs near the magnetic equator; and to provide velocity data for the EPOCS program between TOPS sites.

Prior to this experiment, XCP operations had been at middle and high latitudes only. To learn more about the profiler's limitations in the tropical oceans, XCP profiles taken near the magnetic equator were compared with the velocity profiles obtained using TOPS. From previous mid-latitude work during FRONTS '80 it was known that the two methods (XCP and TOPS) are in good agreement, as shown by Figure 1 (Sanford, 1982). The two profilers agree to within 1-2 cm s^{-1} rms. This performance is typical at mid-latitudes. However, as the XCP is used closer to the equator its performance will degrade because the vertical component of the earth's magnetic field becomes smaller. The aim of the XCP/TOPS comparisons is to determine the extent to which errors increase as the magnetic equator is approached. To understand what effects may be important near the magnetic equator, examine the following simplified form of the equation for the magnetic north velocity component:

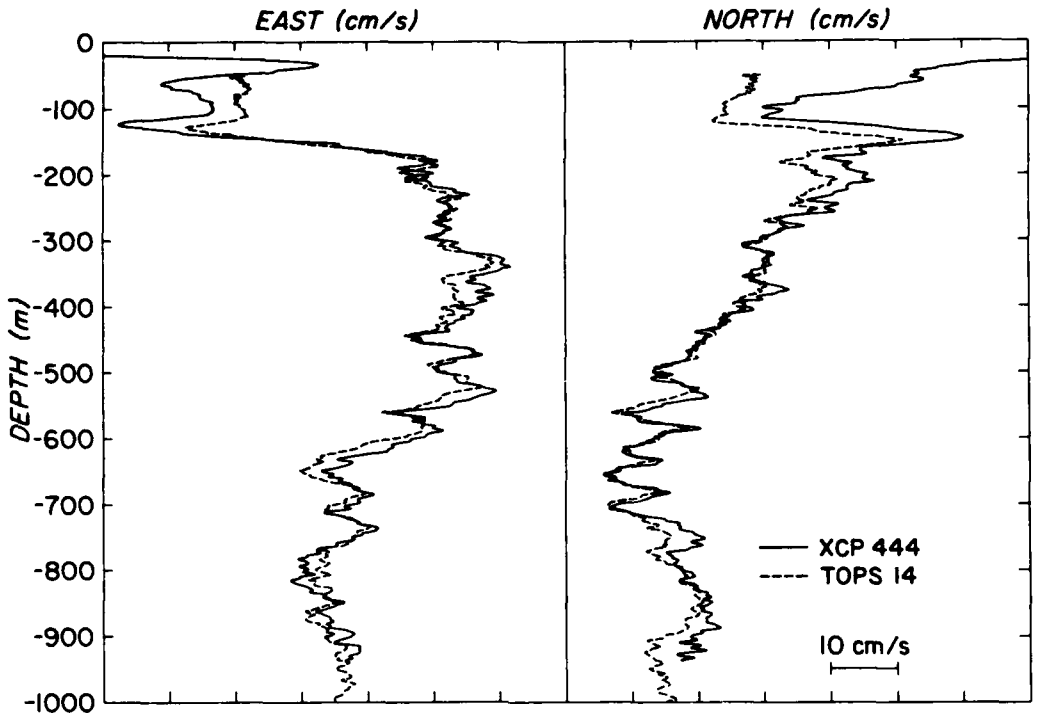

Figure 1. XCP/TOPS velocity comparison during FRONTS '80 experiment, from Sanford (1982). Velocities are in magnetic components.

$$V_{xcp} = v - \bar{v}^{*} + \frac{F_h}{2F_z}\left(W - W' + \frac{v\,H}{L} + \frac{N}{l\,F_h}\right),$$

where

V_{xcp}	is the velocity measured by the XCP (m s^{-1}),
v	is the magnetic north component of velocity (m s^{-1}),
$\bar{v}^{*}$	is the conductivity-weighted vertically averaged velocity (m s^{-1}),
F_h and F_z	are the horizontal and vertical components of the earth's magnetic field (T),
W and W'	are the actual and assumed XCP fall rates (m s^{-1}),
H and L	are the vertical and horizontal length scales of the flow (m),
N	is the electrode/electronic noise (V), and
l	is the length of the electrode line (m).

Combined in this equation we have the desired velocity signal ($v - \bar{v}^*$), a fall rate term, a term dependent on the characteristics of the flow, and a noise contribution. The practical conversion of electric into velocity measurements involves approximations. Thus, the $(vH)/L$ term arises as a first-order correction to the zeroth-order approximation. The term multiplied by F_h/F_z is generally small (several centimeters per second) and mostly depth independent — hence is usually neglected. However, as one approaches the magnetic equator, F_z begins to vanish. This causes terms scaled by F_h/F_z to appear larger near the magnetic equator than at mid-latitudes. Thus, differences between the assumed and actual fall rate and electrode/electronic noise contributions will be amplified near the magnetic equator. Also, the term characterizing the flow, H/L, which is neglected at mid-latitudes, may become important in the vicinity of the magnetic equator.

In this report, nearly simultaneous XCP/XCP velocity intercomparison profiles and XCP/TOPS velocity intercomparison profiles are presented. Standard deviations are computed for the XCP/XCP comparisons. The rms differences are computed between XCP and TOPS. A model for the noise is developed and compared with the computed rms differences, and XCP operational limitations are discussed. The sources of errors, inadequate compensation for fall rate, phase differences, and vessel interference are also considered. Some results from another equatorial experiment, Tropic Heat, will also be discussed.

2. THE EXPERIMENT

The *Discoverer* left Callao, Peru, on 24 March 1982. Initial profiling was performed to the east of the Galapagos Islands, where a short N-S section was run at 85°W from 0°40′N to 2°S to investigate the undercurrent observed on the preceding EPOCS cruise. Three XCPs (851-853) were dropped along this transect. Following that, the ship continued to the first section along 95°W, starting at 3°N. Twenty XCP (854-873) profiles were obtained along this meridian between 3°N and 8°S (three of these units had been adapted especially for engineering tests and were not intended for velocity data acquisition). According to global charts, the magnetic equator is near 8°S along this meridian. We had hoped to continue to about 9 or 10°S for an entire traverse of the magnetic equator, but did not because of time constraints. A medical evacuation to the

Galapagos Islands resulted in the loss of nearly three working days. Subsequently, the cruise plan was modified to emphasize completing as much work as possible in the Eastern Pacific where the EPOCS interest was strongest. Nonetheless, it is clear that the profiling was done sufficiently close to the magnetic equator to reveal performance degradation. After the 95°W transect at 8°S, the *Discoverer* continued to work along the equator as it transited to Hawaii. Ten profiles (874-883) were taken at a spacing of about every 5° of longitude. The ship arrived in Honolulu on 27 April after 35 days at sea. Figure 2 presents the stations' positions, and Table 1 summarizes the station particulars. Not included in Table 1 are four XCPs that failed to drop from the delayed release float. New probes were launched in their place.

The TOPS log information is listed in Table 2 for intercomparison. Five moorings were also deployed on this cruise, and thirty-eight CTD/O_2 stations were occupied.

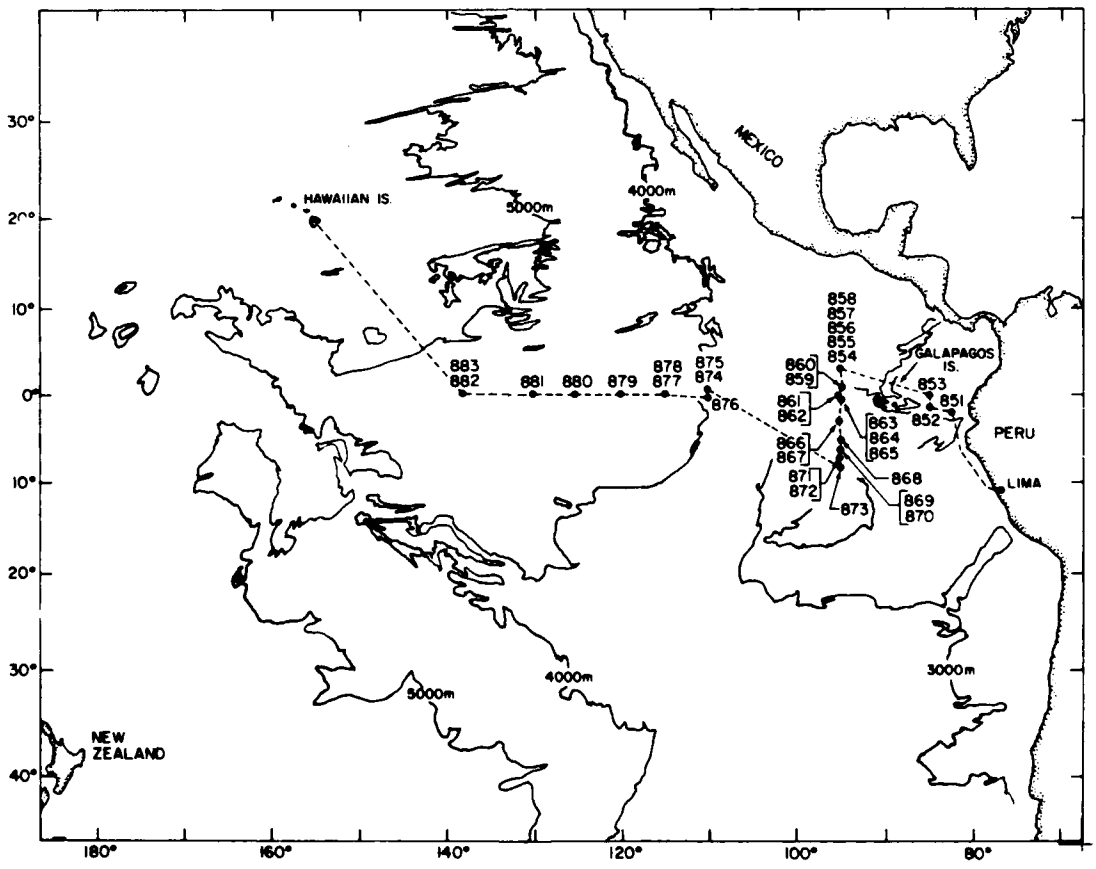

Figure 2. XCP deployment sites during EPOCS cruise. The cruise track is shown by the dashed line.

Table 1. XCP event log (time is GMT).

Drop#	Date	Time	Latitude	Longitude	Comment
851	03/26/82	0059	2 02.6S	82 29.7W	bad east of Galap. I
852	03/28/82	1302	1 24.8S	85 00.7W	good
853	03/29/82	0317	0 03.1S	84 58.4W	good
854	03/30/82	0547	2 58.6N	94 59.6W	shorted
855	03/30/82	0555	2 58.7N	94 59.8W	shorted
856	03/30/82	0625	2 58.7N	95 00.0W	shorted
857	03/30/82	1720	2 59.8N	95 02.2W	good
858	03/31/82	1728	2 59.8N	95 02.2W	fair
859	04/01/82	0714	0 54.5N	94 53.5W	good
860	04/02/82	1704	0 29.3N	95 00.4W	good
861	04/04/82	0856	0 01.9S	95 17.2W	good
862	04/04/82	0905	0 01.2S	95 16.9W	good
863	04/04/82	1822	0 29.1S	95 00.1W	fair
864	04/04/82	2203	0 46.8S	94 58.6W	good
865	04/05/82	0309	1 01.4S	94 58.5W	fair
866	04/09/82	0731	3 00.1S	94 59.6W	bad
867	04/09/82	0743	3 00.7S	94 59.6W	fair
868	04/10/82	1327	5 01.6S	95 00.2W	fair
869	04/10/82	2331	5 59.5S	95 00.2W	poor
870	04/10/82	2342	5 59.5S	95 00.2W	poor
871	04/11/82	1541	7 00.7S	94 59.3W	bad
872	04/11/82	1556	7 00.8S	94 58.9W	poor (F_z small)
873	04/12/82	0532	7 59.8S	94 59.5W	poor (F_z small)
874	04/16/82	0323	0 31.6N	109 55.5W	poor
875	04/16/82	0805	0 04.5N	109 53.2W	good
876	04/16/82	1717	0 30.5S	109 56.2W	good
877	04/17/82	2121	0 00.8N	114 57.1W	bad
878	04/17/82	2141	0 00.8N	114 57.1W	good
879	04/18/82	1935	0 00.2N	119 59.9W	poor
880	04/20/82	1735	0 00.3N	124 59.2W	fair
881	04/20/82	1750	0 00.9S	130 07.9W	good
882	04/22/82	0357	0 00.2N	137 57.2W	good
883	04/22/82	0407	0 00.2N	137 57.2W	poor

Table 2. TOPS event log (time is GMT).

Drop#	Date	Latitude	Longitude
1	3/26/82	2 02.6S	82 29.7W
2	3/28/82	1 24.4S	85 00.7W
3	3/28/82	0 40.0S	85 00.1W
4	3/28/82	0 03.8S	84 58.4W
5	3/29/82	0 41.0N	85 00.6W
6	3/29/82	2 59.8N	95 02.2W
7	4/01/82	2 00.5N	95 00.2W
8	4/01/82	1 30.5N	95 00.3W
9	4/02/82	0 54.5N	94 53.5W
10	4/02/82	0 29.4N	95 00.4W
11	4/02/82	0 01.9S	95 18.1W
12	4/04/82	0 29.1S	95 00.1W
13	4/05/82	1 01.5S	94 59.9W
14	4/05/82	1 30.1S	95 01.8W
15	4/05/82	2 00.7S	94 58.6W
16	4/05/82	2 31.9S	95 01.0W
17	4/09/82	3 00.1S	94 59.6W
18	4/09/82	3 29.5S	95 00.7W
19	4/10/82	3 56.1S	95 03.1W
20	4/10/82	4 29.7S	94 59.4W
21	4/10/82	5 01.5S	95 00.2W
22	4/10/82	5 30.7S	95 00.3W
23	4/11/82	5 59.5S	95 01.4W
24	4/11/82	6 31.3S	94 59.5W
25	4/11/82	7 00.7S	94 59.4W
26	4/11/82	7 28.7S	95 01.0W
27	4/12/82	7 59.6S	94 59.6W
28	4/16/82	0 04.4N	109 53.3W
29	4/19/82	0 00.2N	124 59.2W
30	4/22/82	0 00.2N	137 57.9W

3. INSTRUMENTATION

The XCP, formerly known as the XTVP (Sanford *et al.*, 1980), is a ship-launched expendable instrument that measures a vertical profile of the relative horizontal velocity and temperature. Velocity determinations are based on the principles of electromagnetic induction which govern the weak electric currents induced by the motion of seawater through the earth's magnetic field. The resulting electric current profile corresponds to the velocity profile (offset by an unknown but depth-independent constant, $\bar{v}^*$).

The Mod 6 XCP probe is housed in a Sippican XBT tube. It is deployed with a Sippican hand launcher and a LEXAN tube. The probe descends through the water and transmits signals to the shipboard receiver via a wire link (XBT wire). Three signals are sent to the receiver: electric field, compass direction, and temperature.

The XCP receiving system (Figure 3) consists of a digital receiver (developed by Robert Drever, APL-UW) which receives, amplifies, demodulates, and digitizes the incoming signals for direct computer storage. The computer used for this system is an HP9845B, with an HP9885M flexible disk drive and an HP9872A plotter. The compass information from the probe and the analog electric field signal are available at front panel connectors of the receiver during deployment. The compass signal is used as a reference for a PAR 129A two-phase vector lock-in amplifier. This amplifier synchronously demodulates the electric field voltage into its in-phase (north-south) and quadrature (east-west) components with respect to the compass signal to produce real-time plots, as the probe is falling, of the "velocities" on an HP7064A two-pen XY recorder. As a backup, the data are also recorded on tape using an HP3964A reel-to-reel tape recorder.

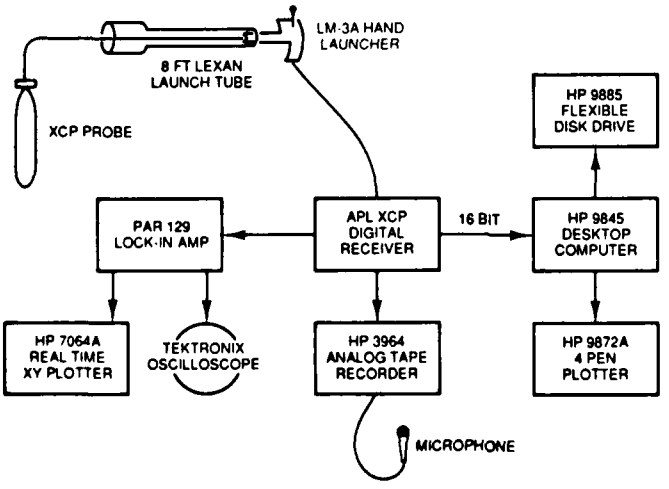

Figure 3.
XCP receiving system.

TOPS is a freely falling profiler (Hayes *et al.*, 1984) that measures vertical profiles of horizontal ocean velocity, conductivity, and temperature. TOPS utilizes acoustic tracking techniques to measure velocity structures at the longer vertical wavelengths ($\lambda > 20$ m) and an onboard, modified, NBIS acoustic velocimeter and magnetometer compass to measure finestructure ($20\text{ m} > \lambda > 20\text{ cm}$). TOPS is tracked acoustically using bottom-mounted transponders that reply to its interrogations. These travel times allow the calculation of an absolute velocity profile based on the acoustically derived positions and time. Additional onboard sensors include two-axis accelerometers, which monitor the motions of the profiler, and an NBIS CTD. All onboard sensors are sampled at 5 Hz; the tracking rate is 0.05 Hz. At the normal fall rate of 0.5 m s^{-1} these sample rates correspond to vertical lengths of 10 cm and 10 m, respectively. Profiling capability extends throughout the full water column (6000 dbar pressure limitation).

A few of the TOPS profiles obtained during this cruise were made absolute using the acoustic tracking techniques. However, in this report we will discuss only the relative TOPS profiles.

4. OPERATIONS

Thirty-seven Sippican Mod 6 XCPs were deployed during the EPOCS cruise. Thirty-two were launched from the *Discoverer*, and five were launched from a rubber boat some distance from the ship. Two probes used floats and ice releases; the remainder used floats and safety fuse releases. Sanford *et al.* (1982) describe the flotation and fuse assembly. The float holds the probe on the surface with the nose pointing upward. When the fuse burns through a nylon line the probe is released from the float, rotates to the nose-down position and begins to fall through the water column. The ship was steaming at 2-3 knots throughout the XCP operations until the wire connecting an XCP to the shipboard receiving system broke. During XCP operations radio silence was maintained.

5. DATA

Of the 37 probes deployed, 29 provided useful data. Four probes failed to drop from their delayed release floats, and an additional four probes yielded bad data (the agar surrounding the electrodes of one of these probes, 851, had dried). Three probes had their electrodes intentionally shorted (854-856) to obtain a measure of the noise sensed by the falling XCP. These probes also provided useful temperature data.

During data acquisition, program DXGET accepts data from the XCP receiver via a 16 bit parallel I/O card (HP98032A) and stores it on floppy disk. The incoming signal is also recorded on audio tape.

Before the actual processing program can be run, it is necessary to estimate the components of the earth's magnetic field, F_h and F_z, at the location of the XCP drop. This is accomplished using PADOC, a program that evaluates a spherical polynomial model based on data and position. Next, the processing program DXPRO takes DXGET files of raw data and produces velocity profiles on files as it plots. The algorithms are described in Sanford *et al.* (1982). DXPRO is usually run with 10 probe revolutions per average and with 5 revolutions between each average.

6. XCP/XCP VELOCITY COMPARISONS

Three pairs of XCPs were dropped within 10 minutes of each other: 857/858, 861/862, and 869/870 (Figure 4a-c). In each panel, the east components of velocity for the XCP pair have been plotted as a function of depth on the left and the north components on the right. The position of the drops and the F_z/F_h ratio are given in the center of the plot.

The standard deviations between these nearly simultaneous drops are summarized in Table 3. The deviation was computed between 200 and 700 m. The upper 200 m was not included in this calculation because of possible contamination by the ship's electric field near the sea surface. Electric currents can exist around the ship because of corrosion and cathodic protection. Sanford *et al.* (1982) discuss contamination of XCP profiles from a vessel's EM fields. For a ship the size of the *Discoverer* they suggest a probe-vessel separation of approximately 150 m at mid-latitudes and more as the magnetic equator is approached. Differences in the upper part of the profiles between simultaneous XCP drops, such as between 857 and 858, are thus attributed to vessel interference resulting from an insufficient separation in distance.

Below 200 m, differences between probes may be attributed either to phase angle differences or fall rate errors. Phase angle differences would be manifested by a depth-independent offset between profiles such as 869/870; fall rate problems would be only in the north component and may be depth dependent. Both of these effects may be enhanced close to the magnetic equator.

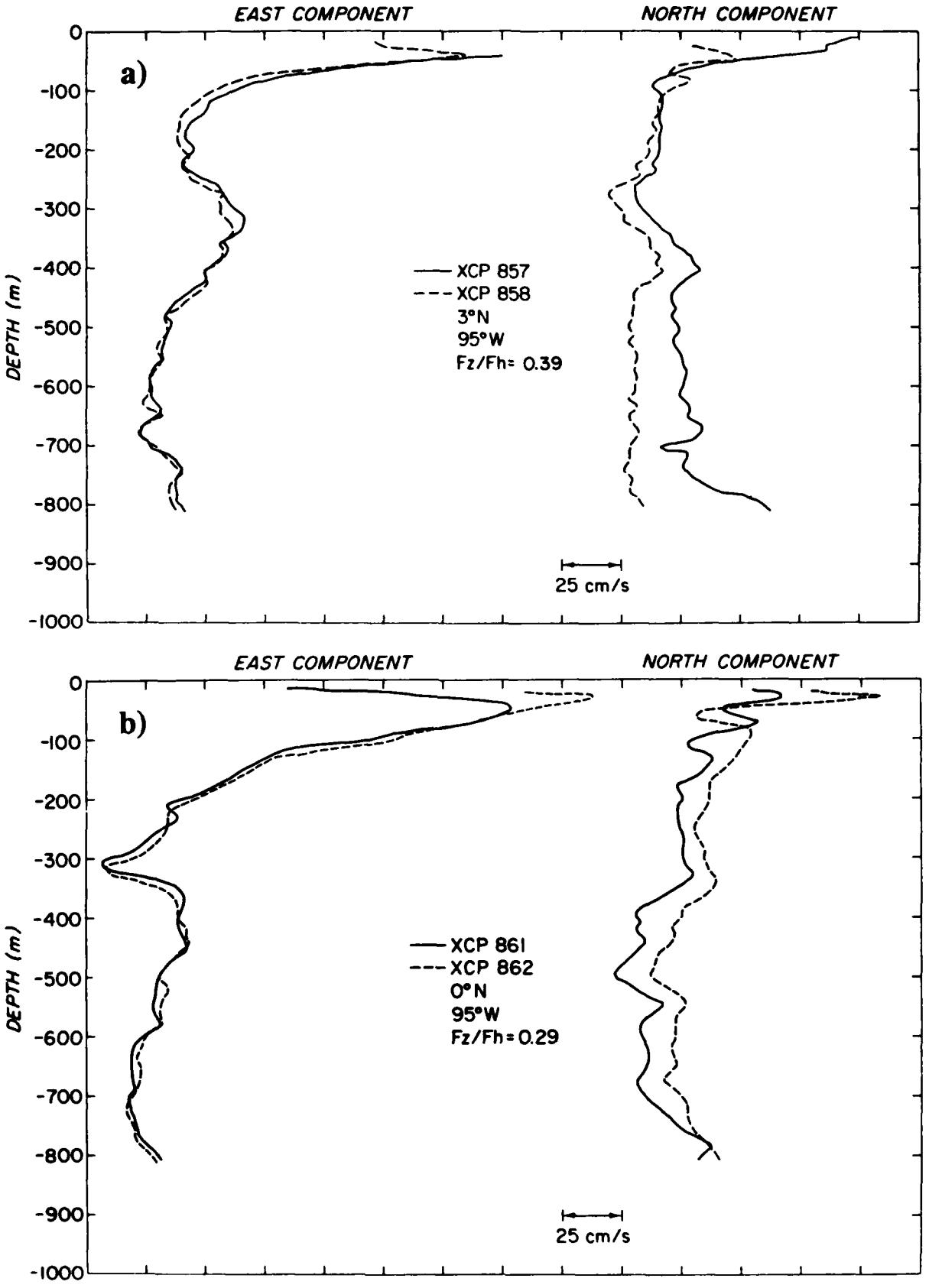

Figure 4a-c. XCP/XCP velocity comparisons. Velocities are in magnetic components.

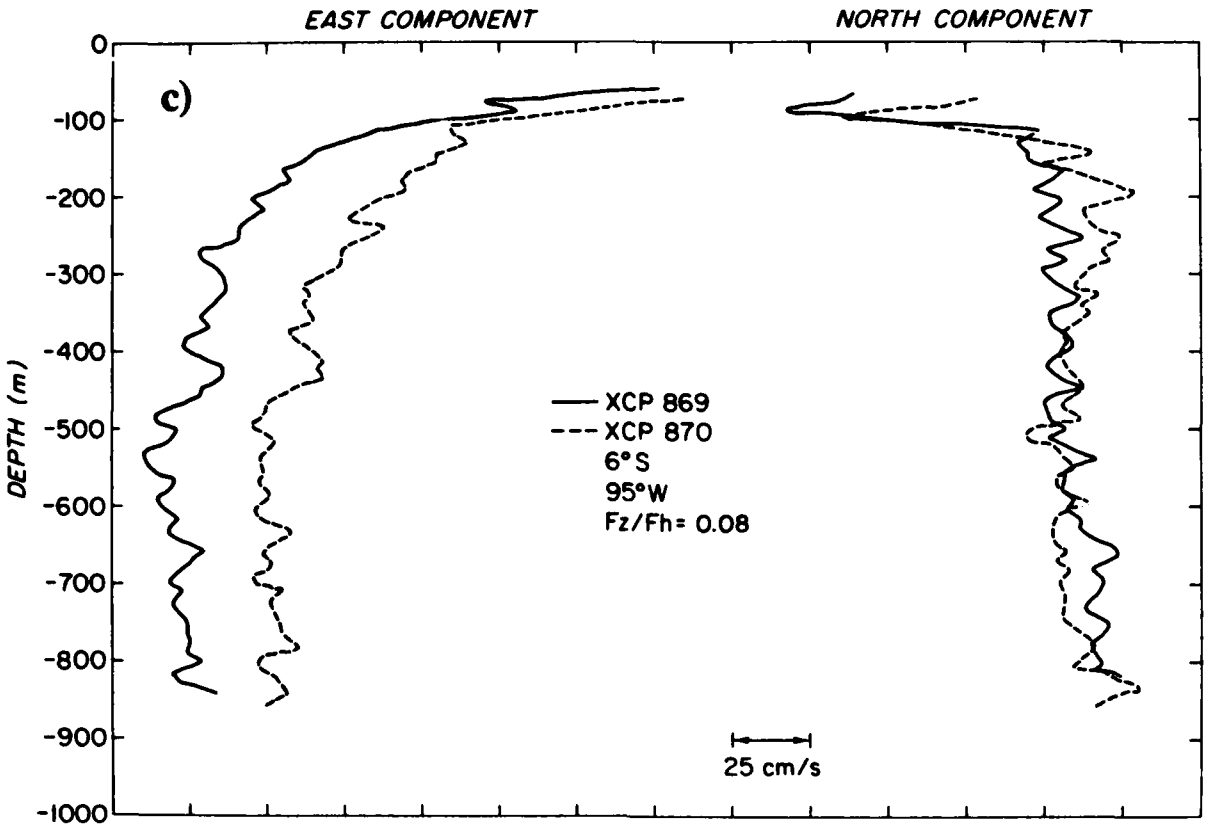

Figure 4. Cont.

Table 3. Standard deviations for XCP/XCP velocity comparisons.

XCP Pair	F_z/F_h	Δt (min)	East (cm s^{-1})	North (cm s^{-1})
857/858	0.39	8	2.5	14.6
861/862	0.29	9	1.8	12.2
869/870	0.08	11	30.6	9.1

To understand the phase angle problem, consider the design criteria for the XCP which was to be able to resolve the desired signal to an uncertainty of 1 cm s^{-1} at mid-latitudes; i.e.,

$$\frac{F_h W \sin\theta}{2 F_z} = 1 \text{ cm s}^{-1} ,$$

where θ is the electrical phase between a signal at the rotation frequency sent separately through the coil and electrode amplifiers. At mid-latitudes $F_h/F_z = 0.5$, so the phase of

the signal relative to the electrode line orientation must be determined to 0.6°. The 0.6° is a specification that is very hard to meet with an expendable probe. The phase error tolerance is improved by mixing a portion of the coil signal with the electric field signal (Drever and Sanford, 1980). The fraction of the coil signal that is added is chosen so that the in-phase and quadrature electric field signals will be of comparable strength. In this case, phase shift uncertainties in the probe and deck equipment can be as large as 6° without degrading the 1 cm s^{-1} performance goal. However, near the magnetic equator where F_z vanishes, small phase differences can produce large uncertainties. For example, the 30.6 cm s^{-1} rms difference between probes 869 and 870, where $F_h/F_z = 12.5$, could be due to a phase difference of 0.6° which is well within the design specifications of 6°.

Profiles 857 and 858 illustrate the problem arising from depth-dependent fall rates (Figure 4a). The differences between these nearly simultaneous profiles are probably due to differences in fall rate or electronic gains. Measurements of fall rate could substantially improve the error situation.

7. XCP/TOPS VELOCITY COMPARISONS

There were 16 stations where both a TOPS drop and an XCP drop were obtained (Figure 5). Fifteen of these provided useful comparisons. The other station, TOPS 2/XCP 852, was not used because of a fall rate problem with the XCP. East and north components of relative velocity have been plotted as a function of depth (Figure 6a-o). The TOPS profile is the solid line in each figure, and the XCP the dashed line. Only the upper 1000 m of the TOPS profiles are shown. Both the XCP and TOPS data shown in Figure 6 are relative, therefore to compare the two instruments, the profiles were shifted in velocity to align major features. No adjustments were made to the depth scales. The position of the drops and the F_z/F_h ratio are given in the center of each plot.

Table 4 lists the rms differences between TOPS and XCP profiles computed between 200 and 700 m. Differences between the two profilers in the upper 200 m are again partly due to contamination of the XCP profile from the vessel's EM fields. Differences below 200 m will be considered in the discussion section where we develop the velocity component equations for the XCP and look at the effect of the vanishing F_z on the individual terms in the equations.

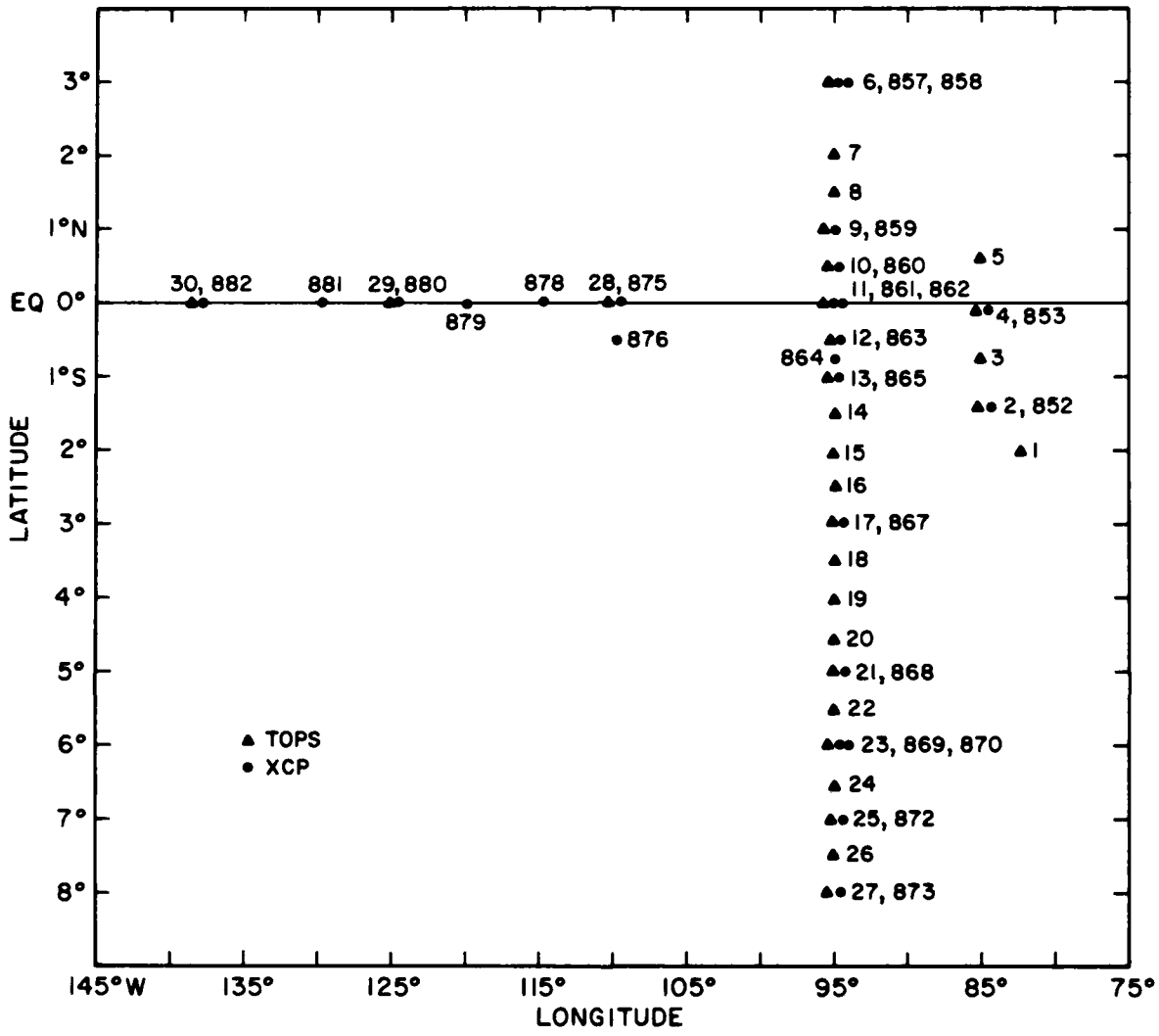

Figure 5. XCP/TOPS positions.

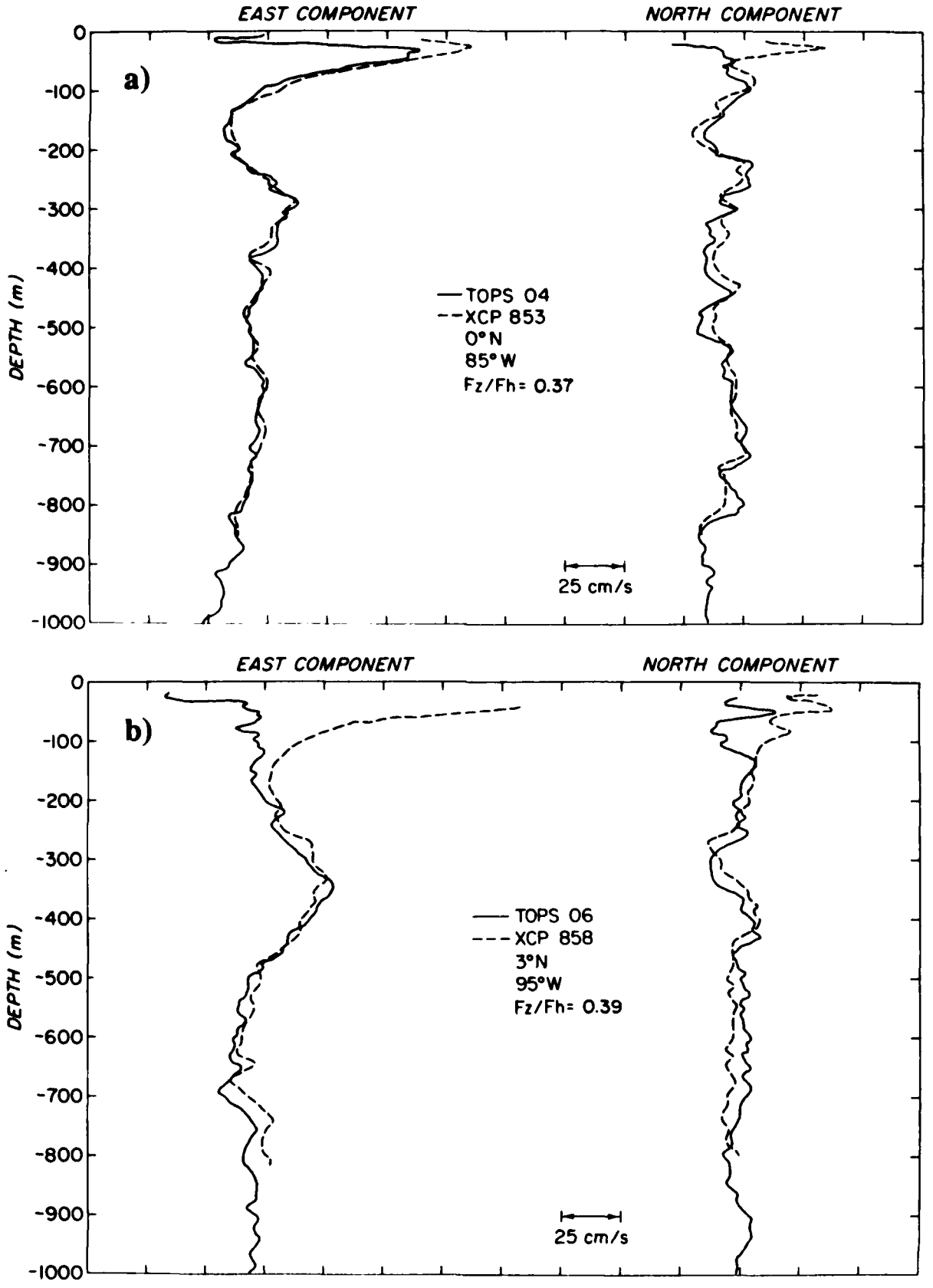

Figure 6a-o. XCP/TOPS velocity comparisons. Velocities are in magnetic components.

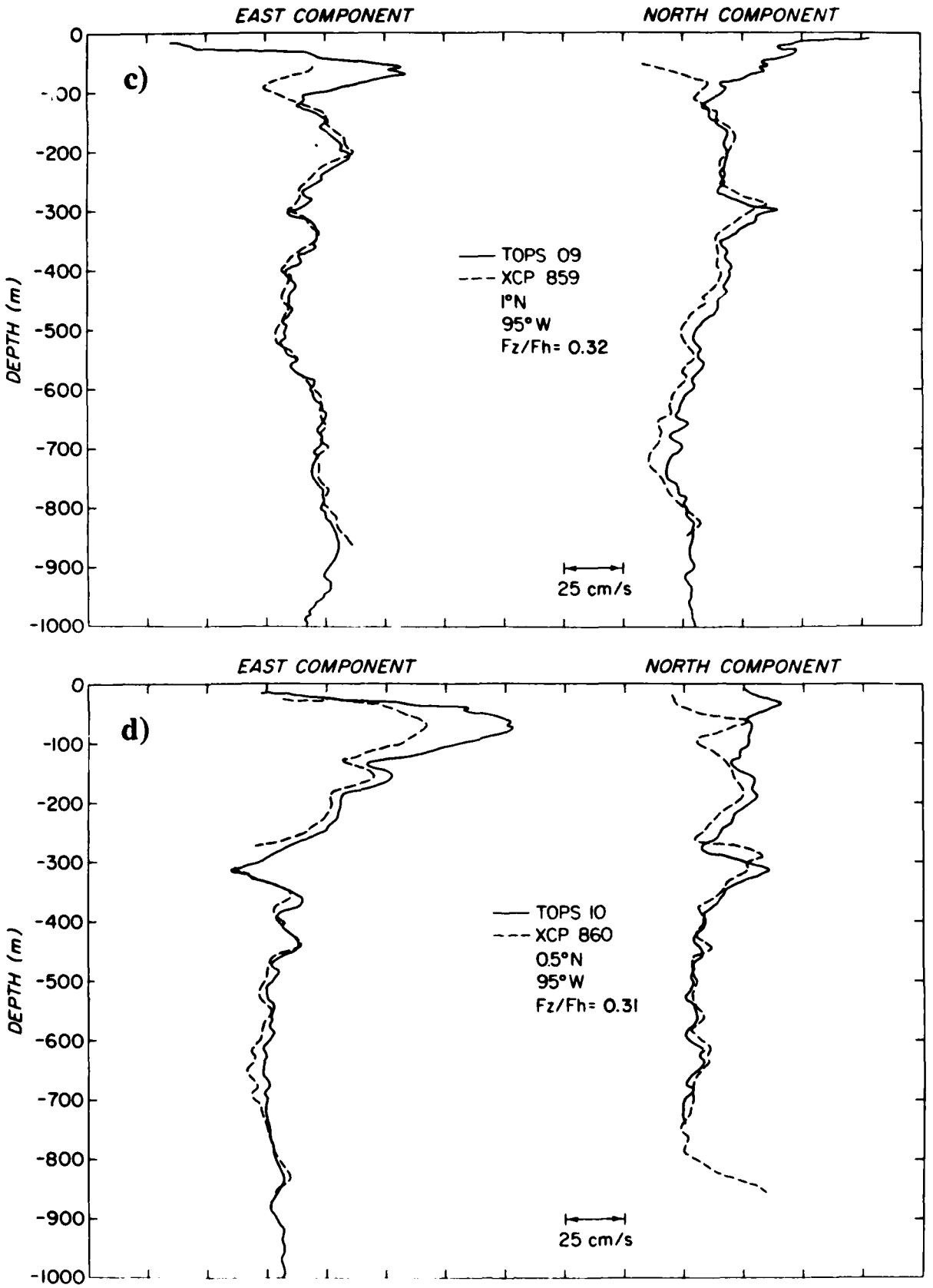

Figure 6. Cont.

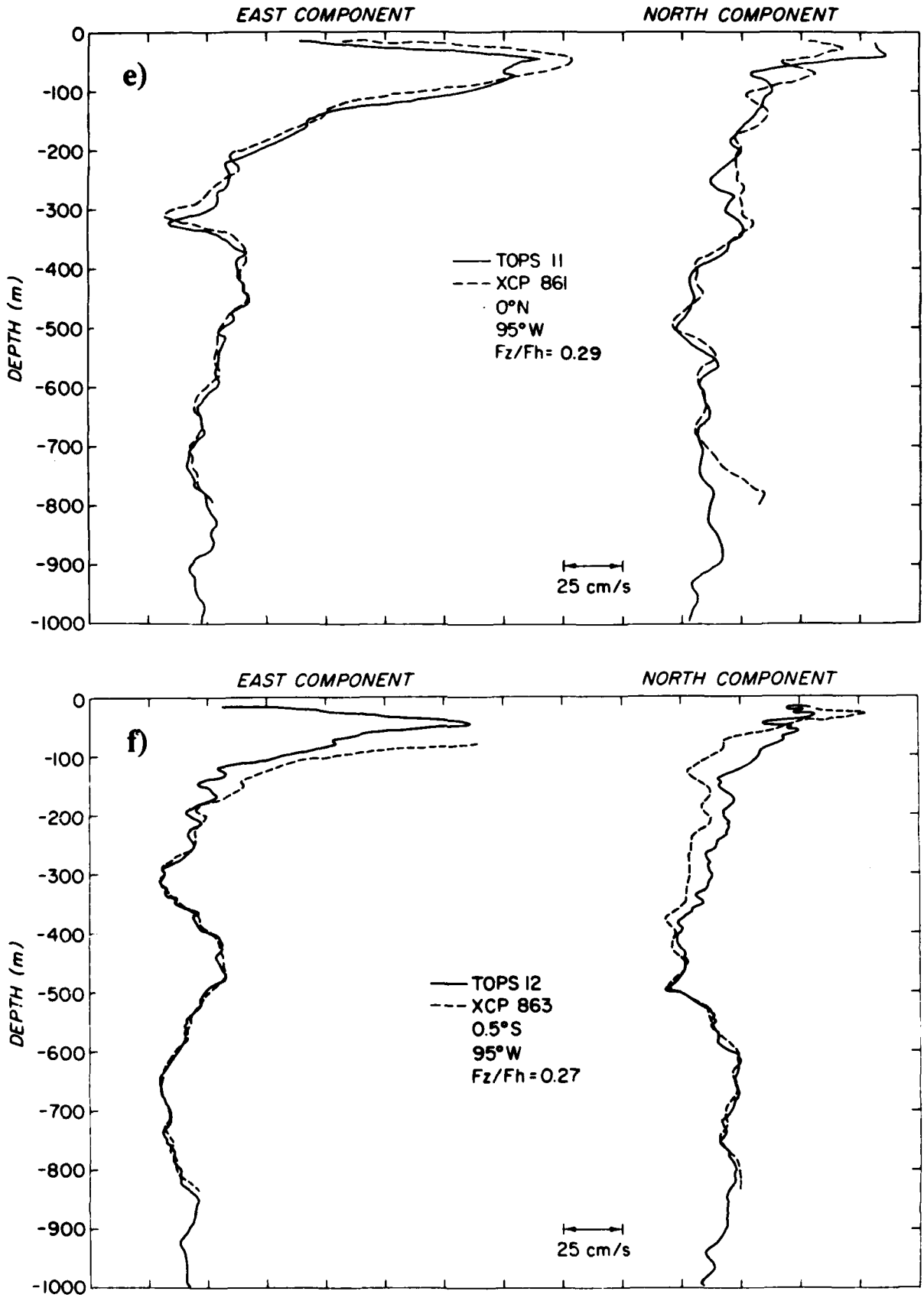

Figure 6. Cont.

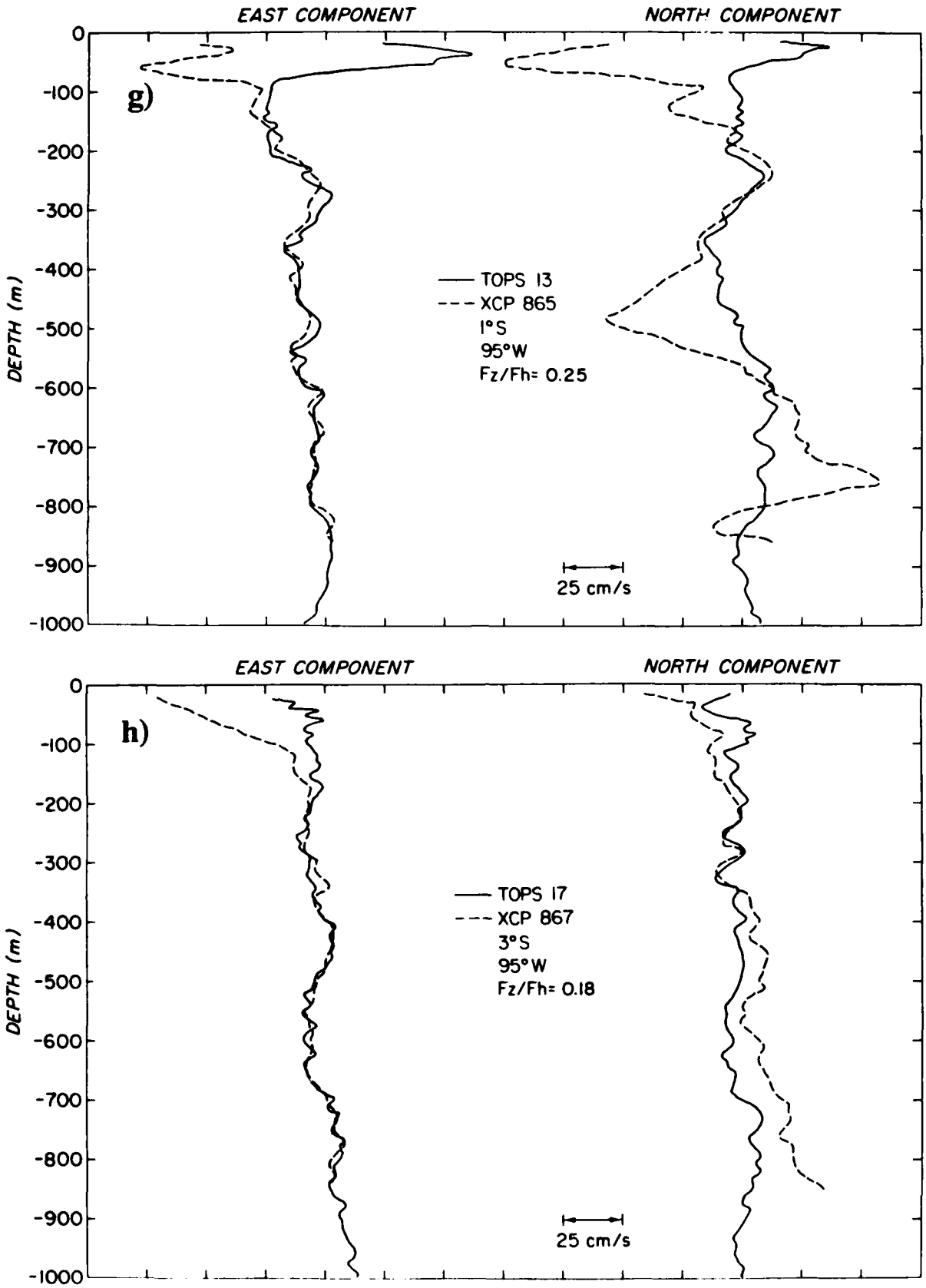

Figure 6. Cont.

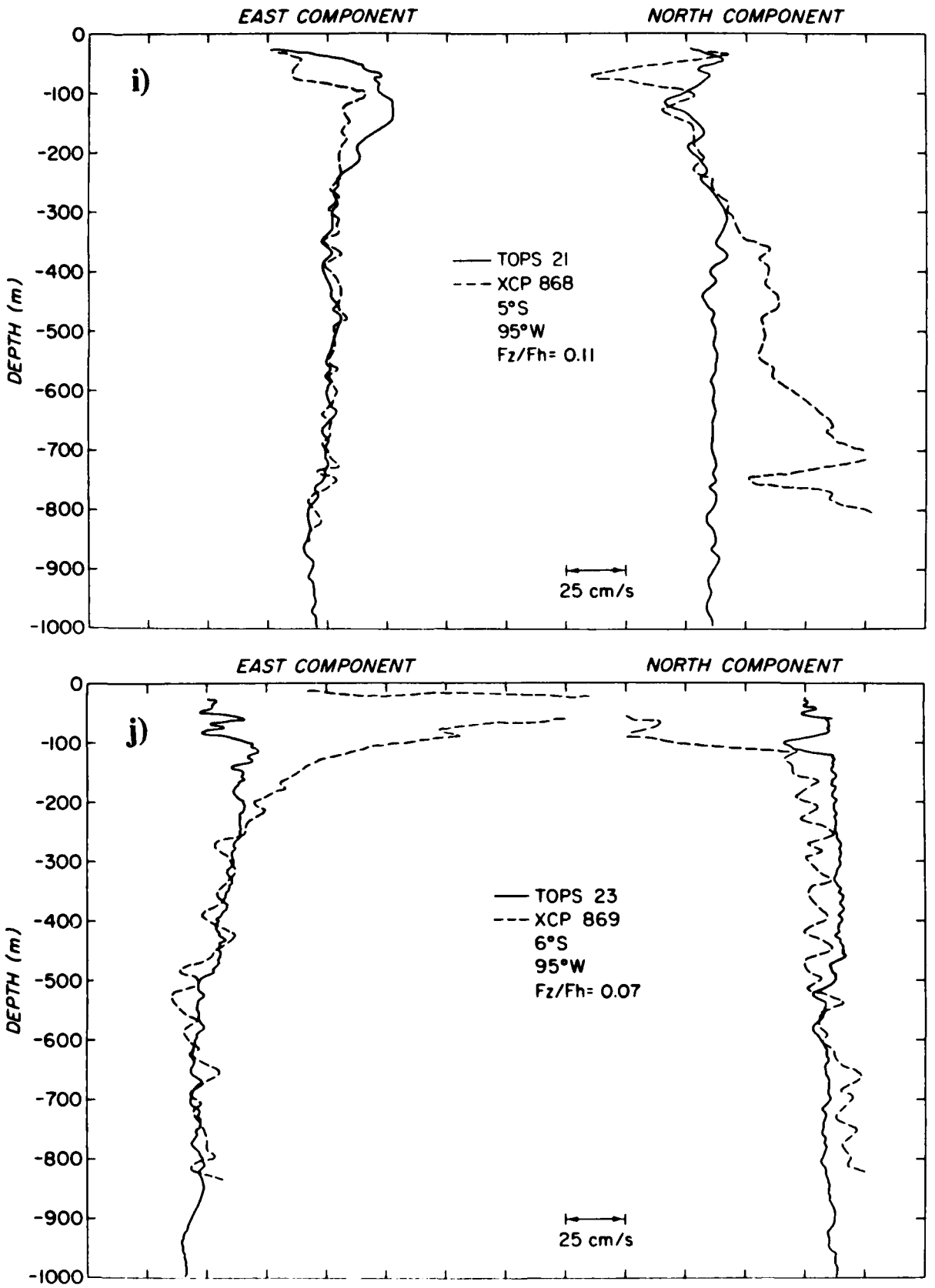

Figure 6. Cont.

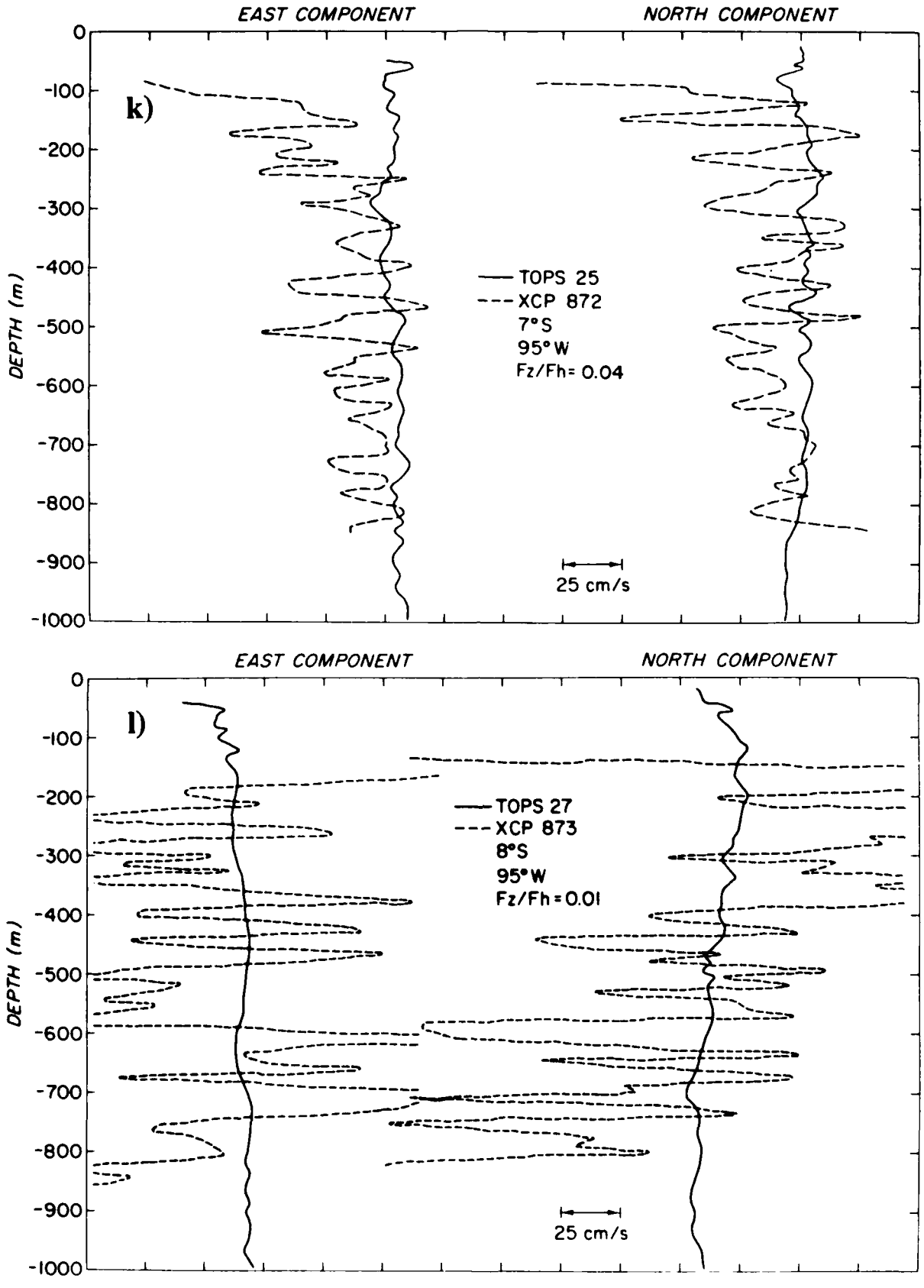

Figure 6. Cont.

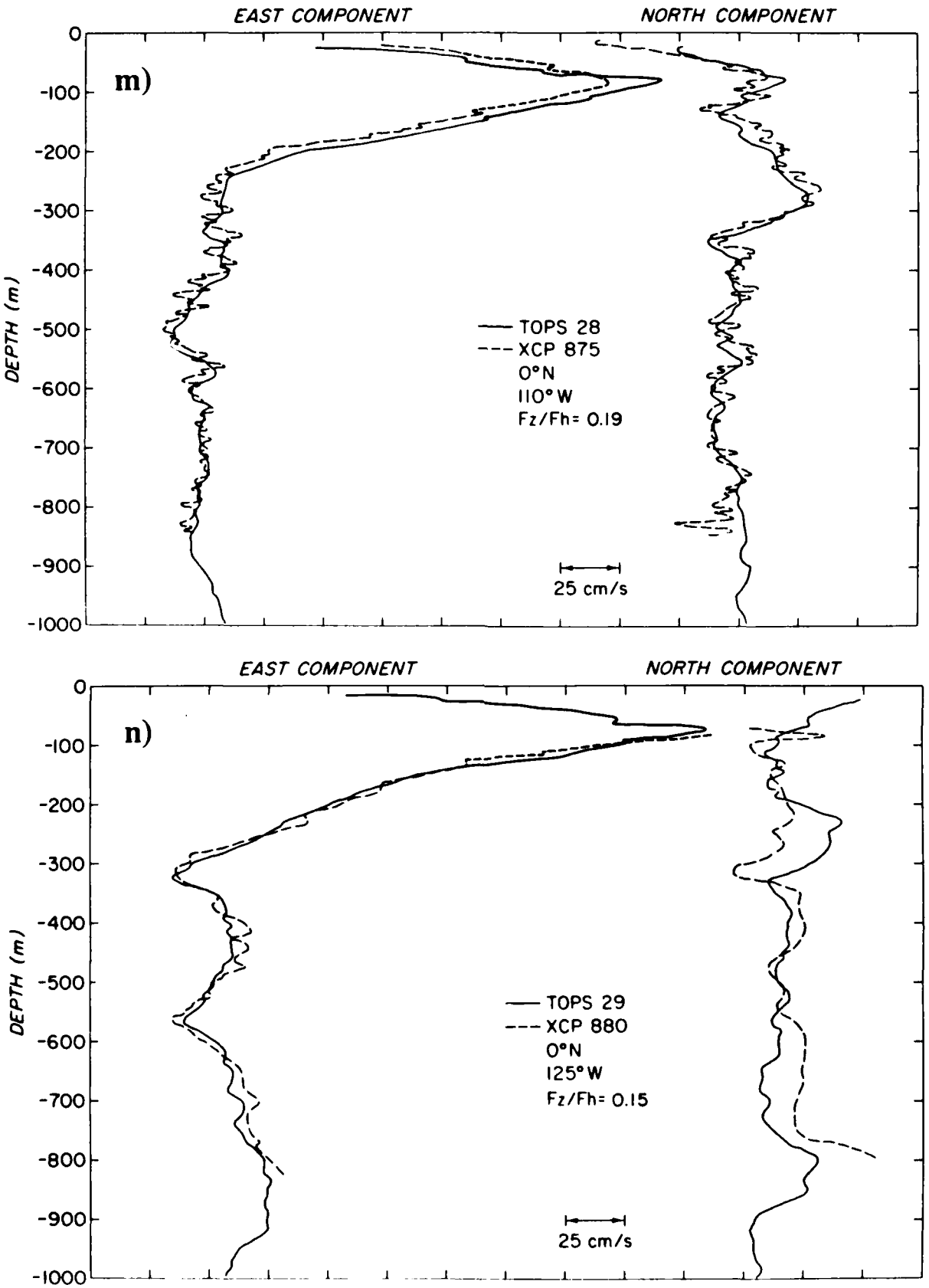

Figure 6. Cont.

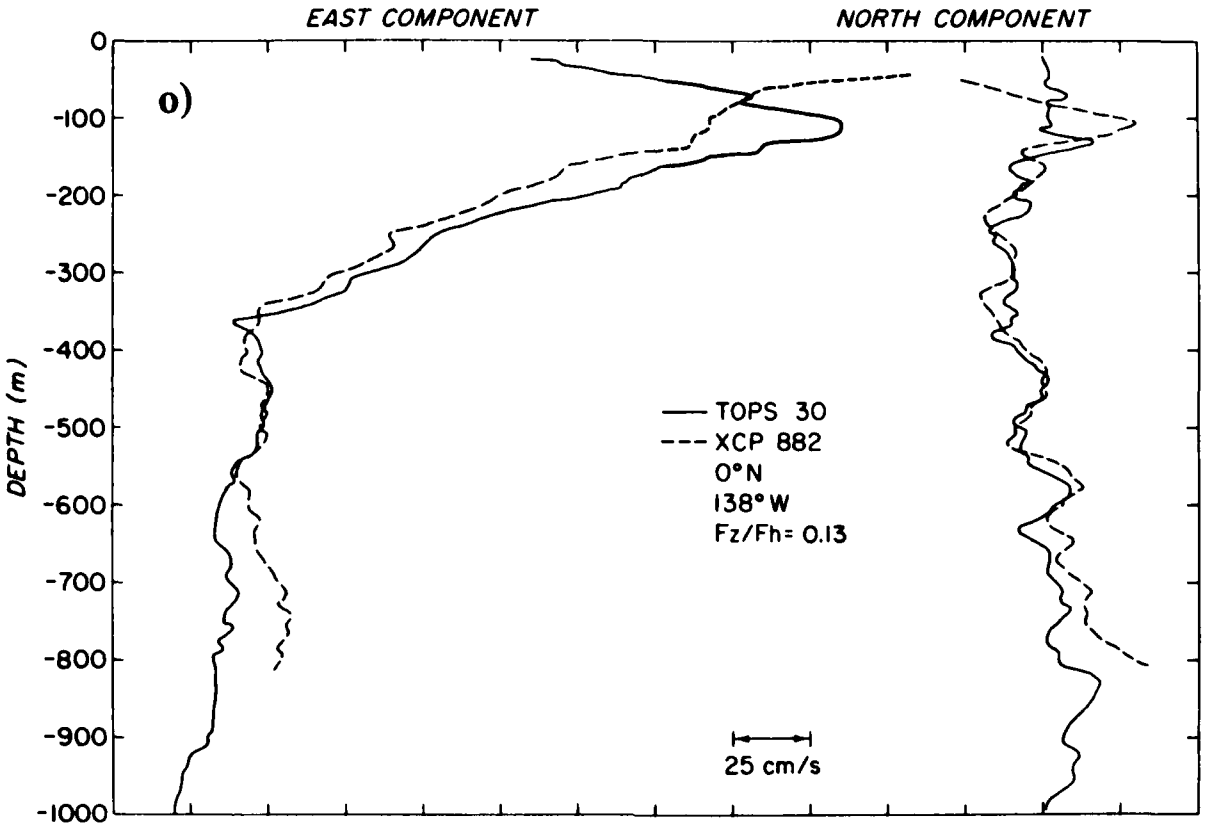

Figure 6. Cont.

Table 4. The rms difference for TOPS/XCP comparisons.

TOPS#	XCP#	F_z/F_h	East (cm s^{-1})	North (cm s^{-1})
4	853	0.37	2	3
6	858	0.39	4	6
9	859	0.32	3	5
10	860	0.31	3	3
11	861	0.29	3	3
12	863	0.27	3	5
13	865	0.25	3	24
17	867	0.18	3	6
21	868	0.11	3	12
23	869	0.07	8	6
25	872	0.04	24	21
27	873	0.01	18	15
28	875	0.19	4	4
29	880	0.15	4	10
30	882	0.13	9	9

8. TEMPERATURE SECTIONS

Sections of temperature measured by the XCP are plotted as a function of depth in Figure 7. The XCP drop number is given below each profile. The leftmost profile is plotted to the temperature scale at the bottom of the plot. All other drops are successively shifted 2°. There are two sections: one along 95°W (Figure 7a), and one along the geographic equator (Figure 7b). Section orientation is given by the directions indicated at the top of the plots.

9. VELOCITY SECTIONS

The magnetic east (u) and north (v) components of relative velocity are plotted as a function of depth in section format in Figure 8a,b. The top panel is the magnetic east component and the lower panel is north. Two sections are shown: one along 95°W (Figure 8a) and a section along the geographic equator (Figure 8b). The leftmost profile is plotted to the scale shown. All other drops are successively shifted over 1.0 m s^{-1}. The drop number is indicated below each profile. Because the performance of the XCP degrades as the magnetic equator is approached, drops 872 and 873 are not included in the 95°W section in Figure 8. To view these two profiles see Figure 6k-l.

10. SHORTED ELECTRODE PROBES

There were three probes, 854, 855, and 856, that had their electrodes intentionally shorted with a salt bridge open on only one end to the surrounding seawater. These three were all deployed at 3°N, 95°W. When the electrodes are shorted the information obtained is essentially noise. This measurement of noise can be used in modeling the expected noise for probes dropped closer to the magnetic equator.

The u and v components for the three probes are shown in Figure 9. The magnetic east component is displayed in the upper panel and the magnetic north in the lower. XCP 854 is plotted to the scale shown; the other two drops are successively shifted over 0.5 m s^{-1}.

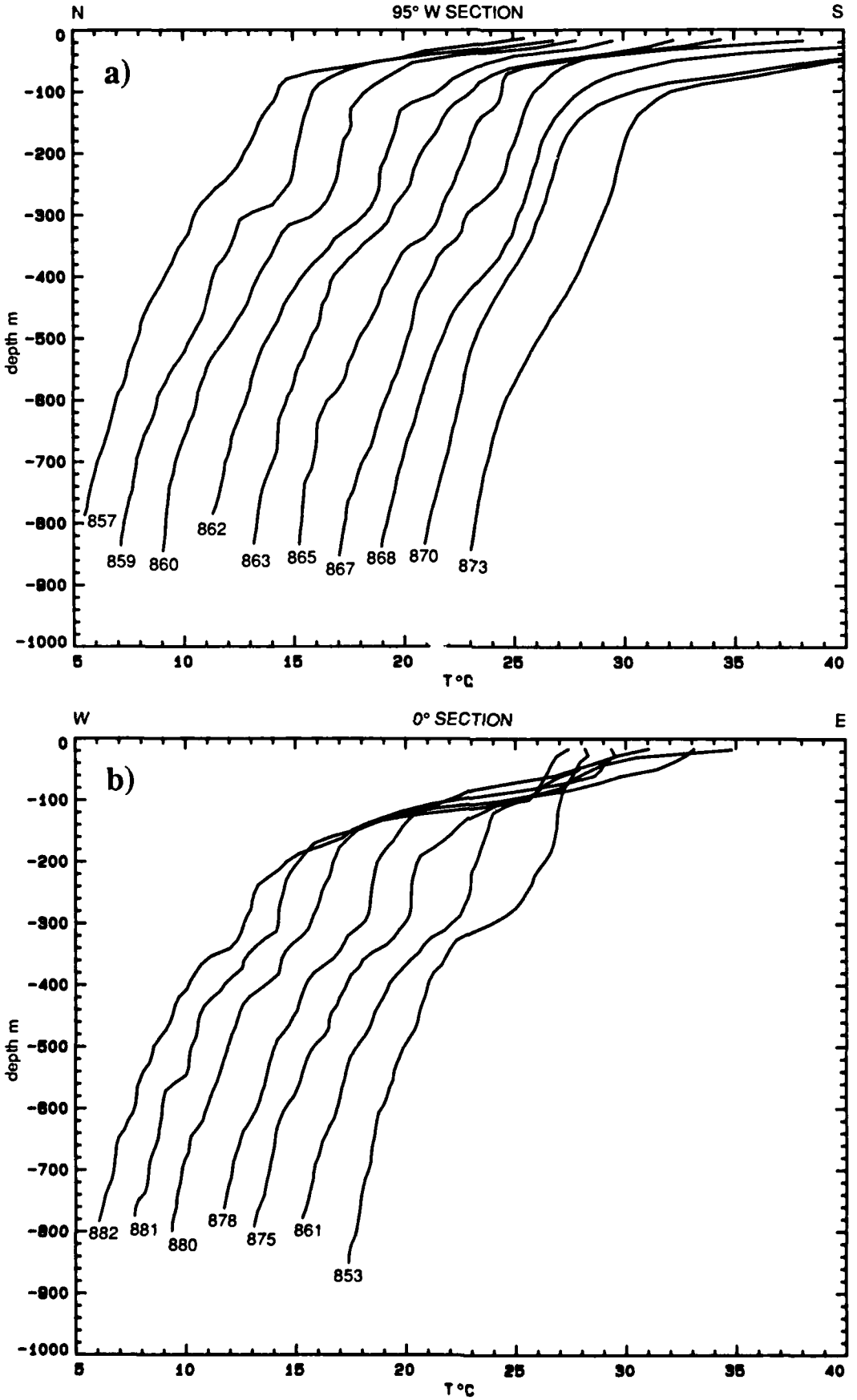

Figure 7a-b. Waterfall sections of temperature.

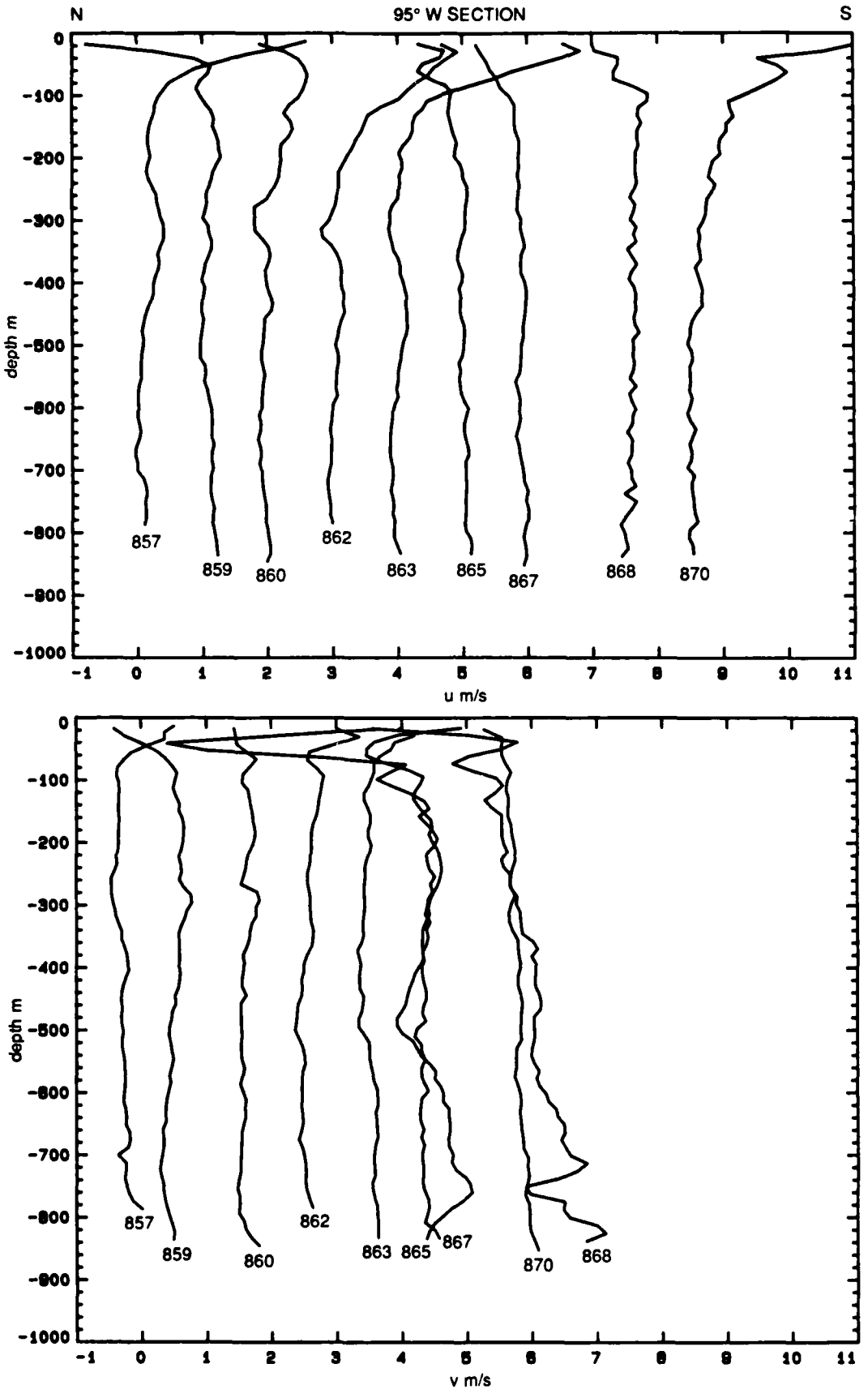

Figure 8a. XCP east (u) and north (v) velocity sections. Velocities are in magnetic components.

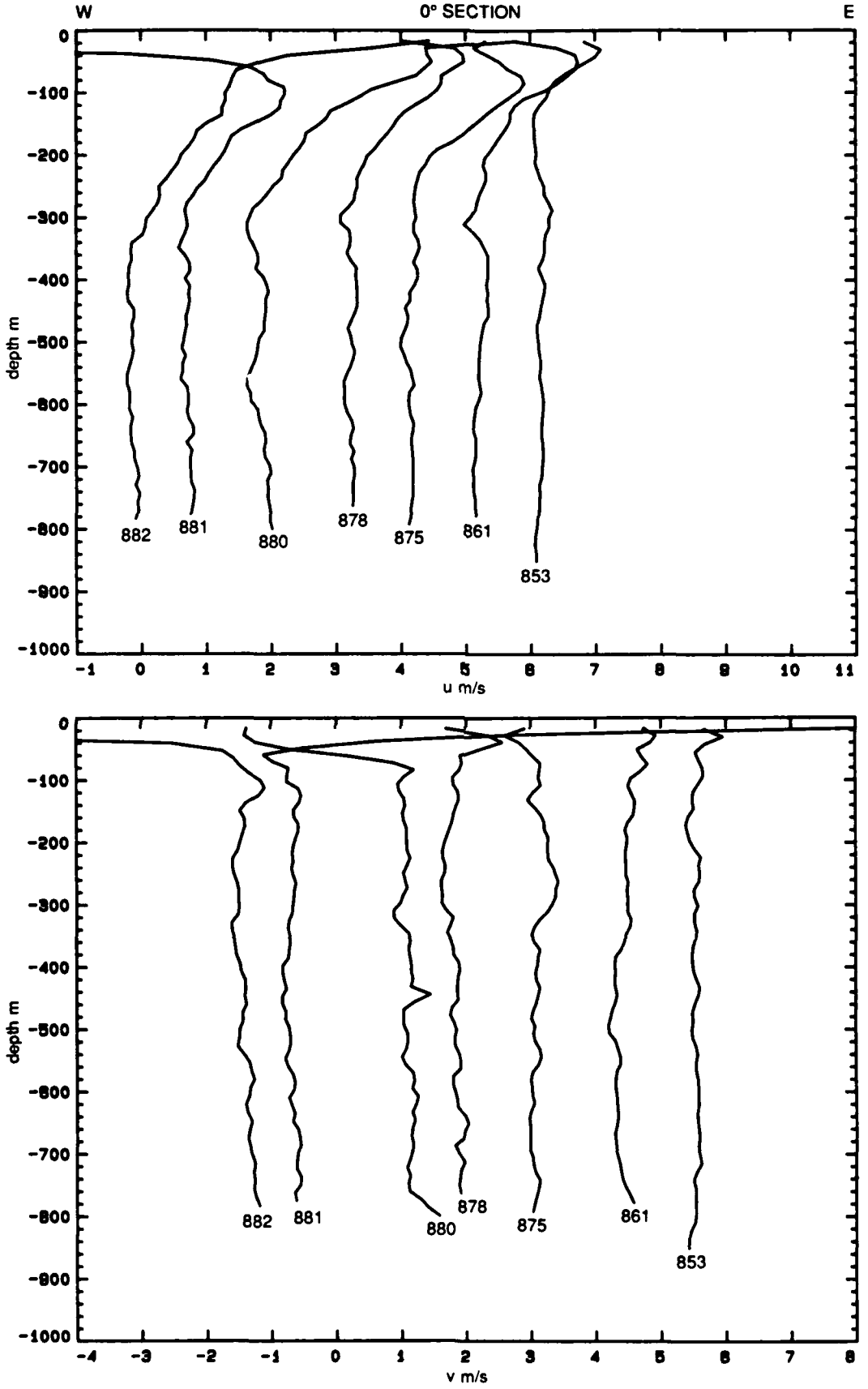

Figure 8b. XCP east (u) and north (v) velocity sections. Velocities are in magnetic components.

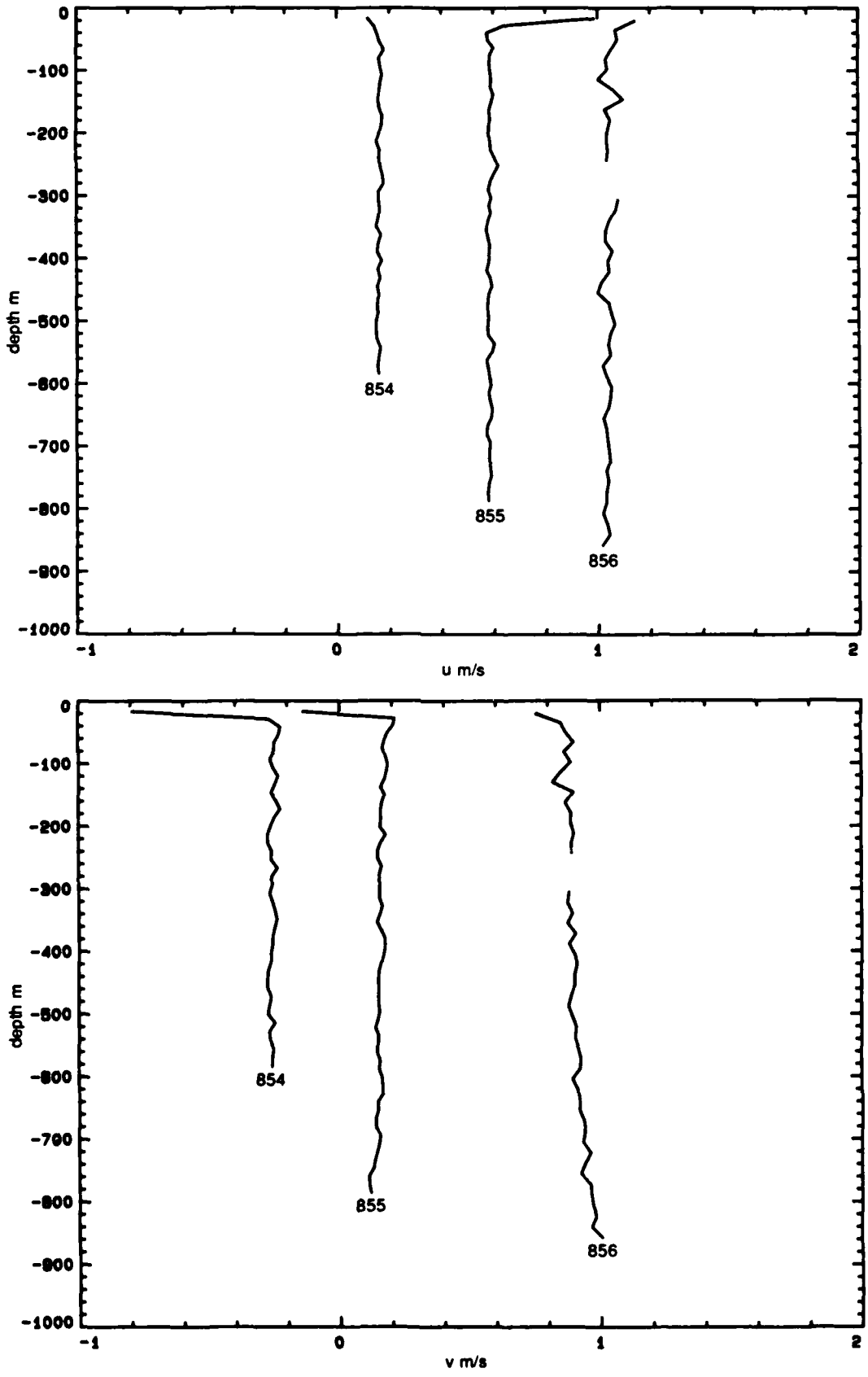

Figure 9. Shorted electrode probes' east (u) and north (v) velocities. These data are a measurement of the noise sensed by the probe.

11. DISCUSSION

The noise level of the XCPs increased as the magnetic equator was approached (Figure 10a-c) because the electrode and electronic noise are independent of the motional electric fields in the sea and, hence, the noise increases in comparison with the signal. In addition, fall rate errors, phase angle differences, and vessel interference effects are magnified near the magnetic equator. To see this more clearly, consider the following expression for the potential difference, $\Delta\phi$, formed from the potential difference at the electrodes, plus a potential difference equivalent to that contributed by the coil signal from the mixer circuit, plus the computed fall rate compensation:

$$\Delta\phi = \Delta\phi^E + \Delta\phi^M - \Delta\phi^W ,$$

where $\Delta\phi^E$ denotes the electrode contribution, $\Delta\phi^M$ the mixer contribution (fraction of compass coil signal), and $\Delta\phi^W$ the fall rate compensation. Separating the in-phase (north-south) and quadrature (east-west) components,

$$\Delta\phi_{in-phase} = \Delta\phi^E_{in-phase} - \Delta\phi^E_{quad} \sin\theta + \Delta\phi^M - \Delta\phi^W_{in-phase}$$

and

$$\Delta\phi_{quad} = \Delta\phi^E_{quad} + \Delta\phi^E_{in-phase} \sin\theta .$$

The $\sin\theta$ term enters into the equations if there is a phase angle between the electric field channel (i.e., $\Delta\phi^E - \Delta\phi^W$) with respect to the coil channel (i.e., $\Delta\phi^M$) .

$$\Delta\phi^E_{in-phase} = F_z\, l\, (1 + C_1)\, (v - \bar{v}^{\,*}) + V_n + F_h\, l\, (1 + C_2)\, W ,$$

$$\Delta\phi^E_{quad} = F_z\, l\, (1 + C_1)\, (u - \bar{u}^{\,*}) + U_n ,$$

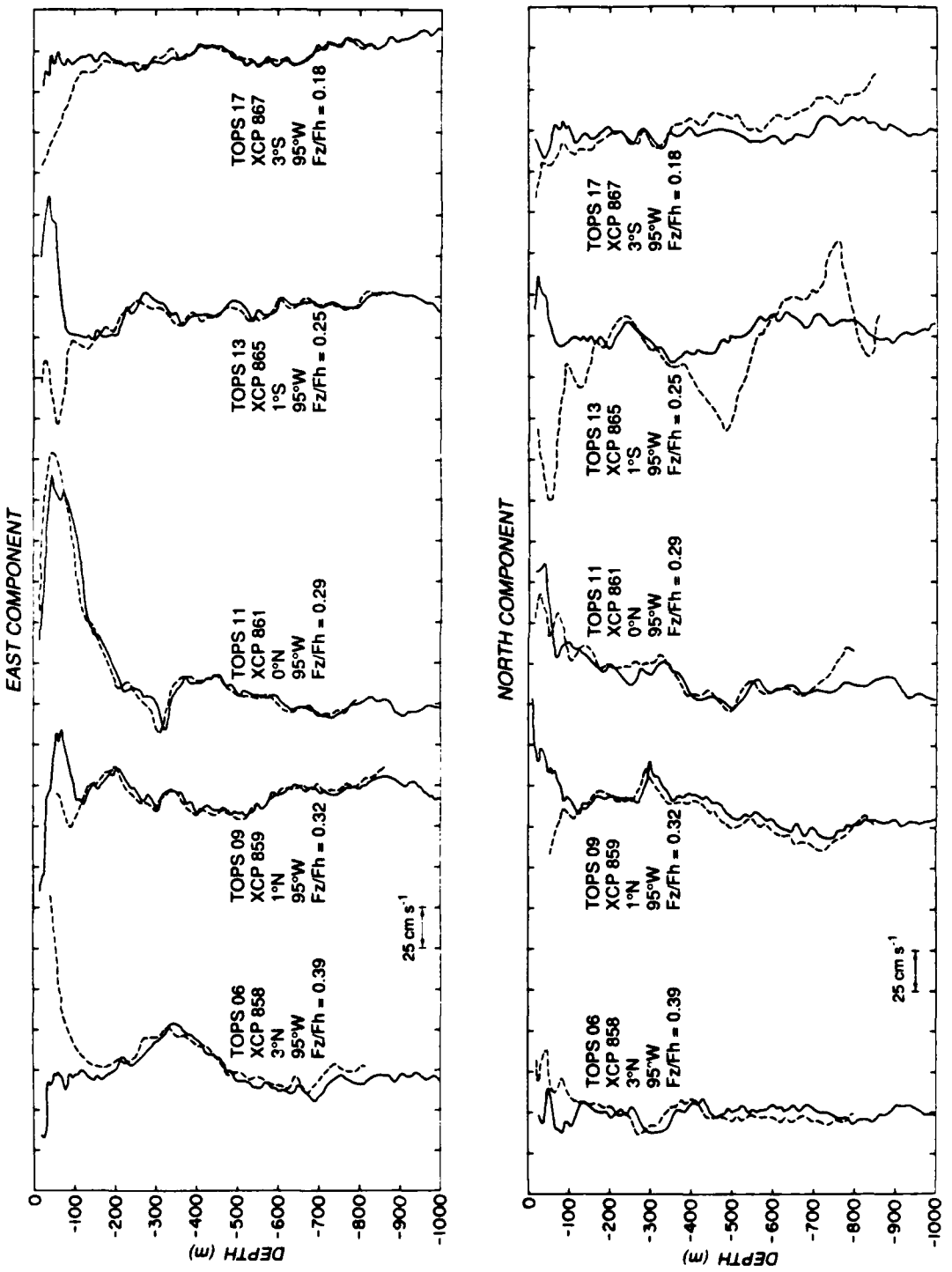

Figure 10a. XCP/TOPS east and north velocity comparison, 95°W section 3°N to 3°S. TOPS profiles are solid lines, XCPs are dashed.

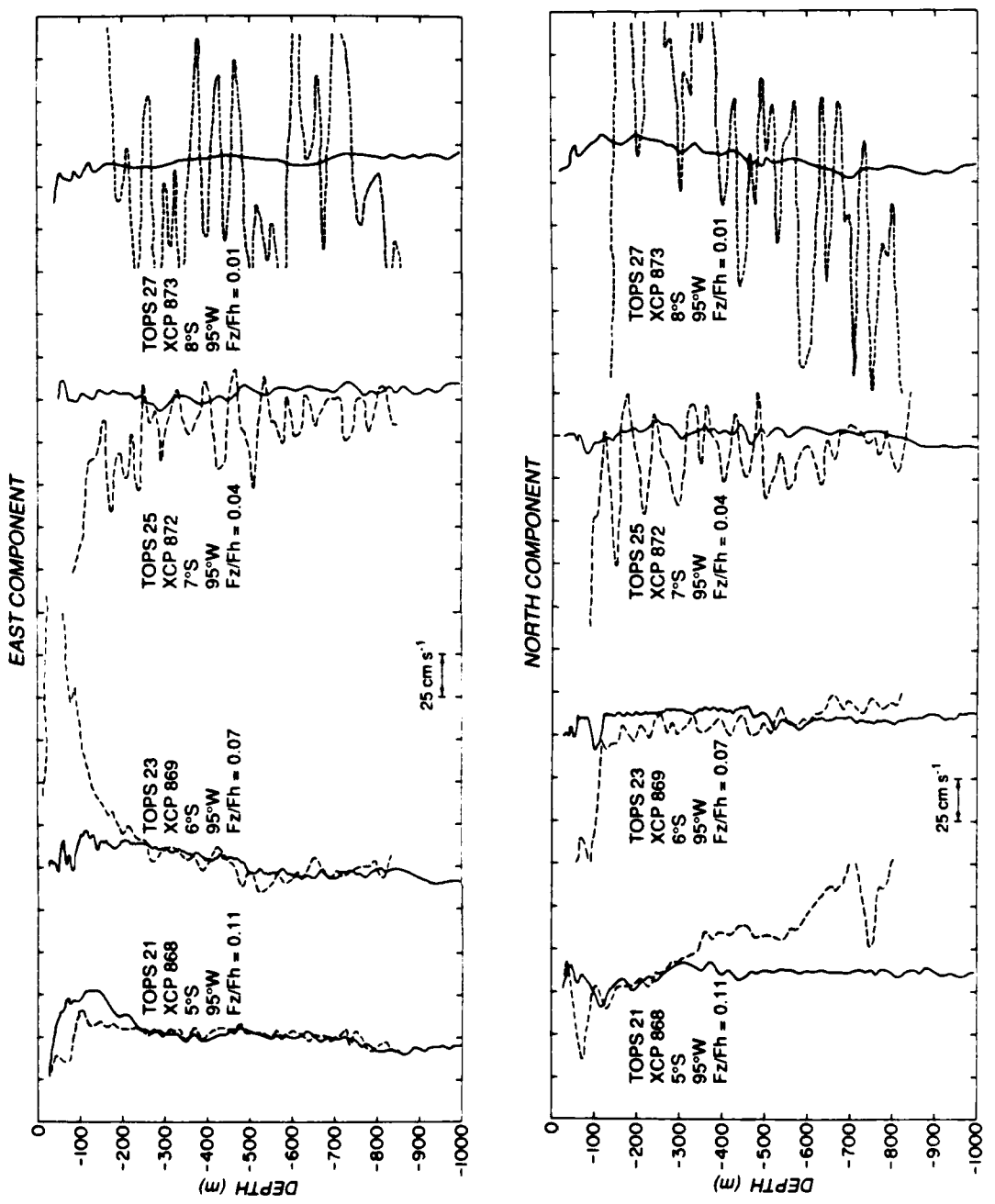

Figure 10b. XCP/TOPS east and north velocity comparison, 95°W section 5°S to 8°S. TOPS profiles are solid lines, XCPs are dashed.

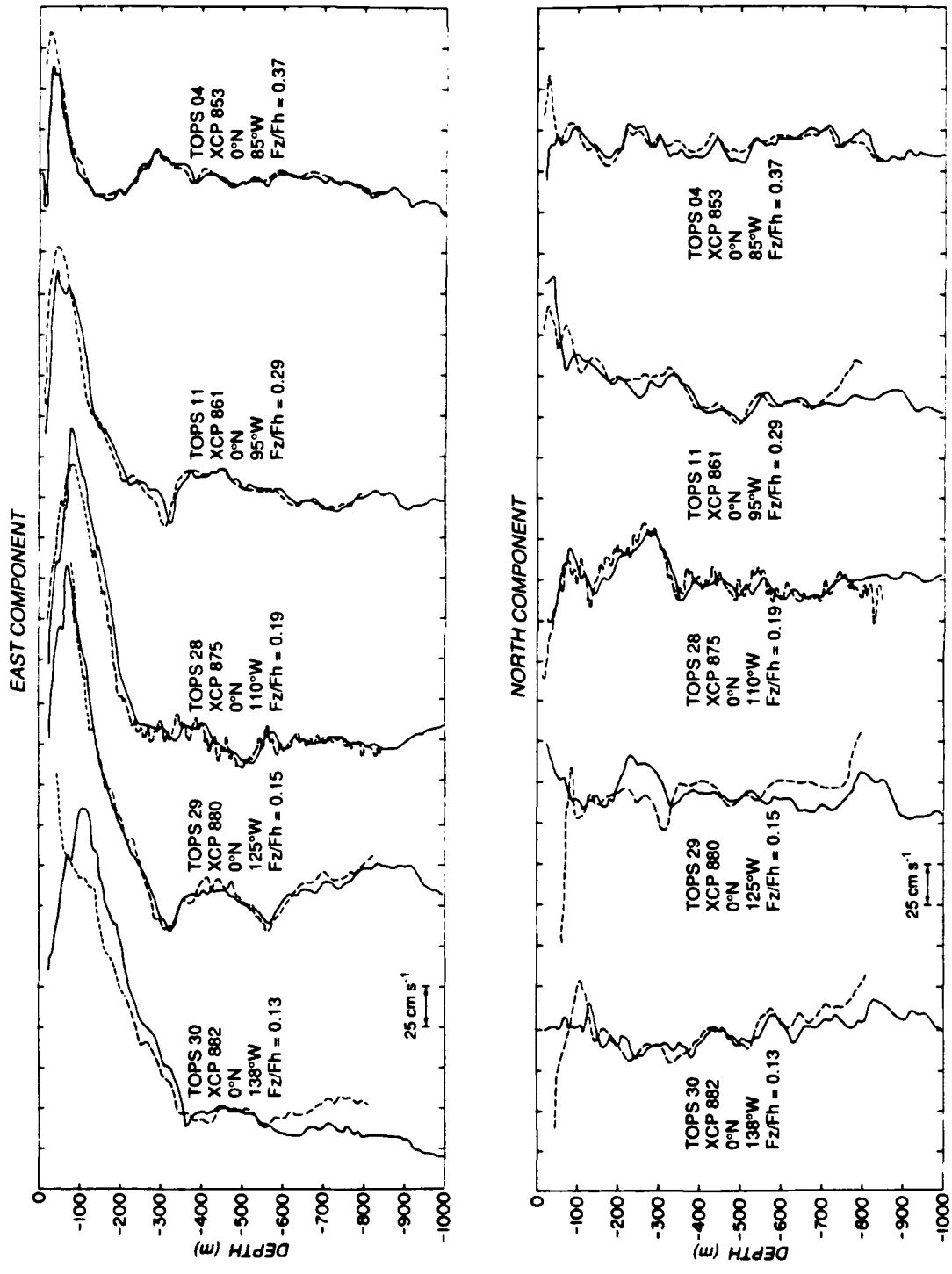

Figure 10c. XCP/TOPS east and north velocity comparison, equator section 138°W to 85°W. TOPS profiles are solid lines, XCPs are dashed.

$$\Delta\phi^M = F_h\, \omega\, n\, A\, C_3,$$

$$\Delta\phi^W = F_h'\, l'\, (1 + C_2)'\, W' + F_h\, \omega\, n\, A\, C_3',$$

where

$'$ (prime)	denotes an assumed or computed value,
F_h and F_z	are the horizontal and vertical components of the earth's magnetic field,
l	is the length of the electrode line (5 cm),
C_1 and C_2	are scale factors depending on the shape of the probe (thought to be 0.9 and -0.02 respectively),
$u - \bar{u}^*$ and $v - \bar{v}^*$	are the east and north horizontal velocity components,
U_n and V_n	are the electrode/electronic processing noise taken to be independent of the signals in the ocean ($\simeq 4.3$ m s^{-1}),
W	is the vertical component of velocity (negative value for falling probe),
ω	is the rotation rate of the probe ($\simeq 7$ Hz),
nA	is the effective area of the coil times the number of turns,
C_3	is the fraction of the coil signal added to the electric field signal ($\simeq 0.04$), and
$F_h\, \omega\, n\, A$	is the signal of the compass coil independently measured.

Combining terms,

$$\Delta\phi_{in-phase} = F_z\, l\, (1 + C_1)\, (v - \bar{v}^*) + V_n + F_h\, l\, (1 + C_2)\, W$$

$$- \left[F_z\, l\, (1 + C_1)\, (u - \bar{u}^*) + U_n\right] \sin\theta$$

$$+F_h\,\omega\,n\,A\,C_3 - F_h'\,l'\,(1+C_2)'\,W' - F_h\,\omega\,n\,A\,C_3'$$

and

$$\Delta\phi_{quad} = F_z\,l\,(1+C_1)\,(u-\bar{u}^*) + U_n$$

$$+\left[F_z\,l\,(1+C_1)\,(v-\bar{v}^*) + V_n + F_h\,l\,(1+C_2)\,W\right]\sin\theta\,.$$

The data processor determines the in-phase and quadrature components of $\Delta\phi$ and computes the velocity components based on the measurements, the assumed calibrations, and the assumed magnetic field components. The assumed values have been denoted with a prime. Then the north and east XCP velocity components are

$$v-\bar{v}^* = \frac{F_z\,l\,(1+C_1)\,(v-\bar{v}^*)}{F_z'\,l'\,(1+C_1)'} + \frac{V_n}{F_z'\,l'\,(1+C_1)'} + \frac{F_h\,l\,(1+C_2)\,W}{F_z'\,l'\,(1+C_1)'}$$

$$-\frac{\left[F_z\,l\,(1+C_1)\,(u-\bar{u}^*) + U_n\right]\sin\theta}{F_z'\,l'\,(1+C_1)'}$$

$$+\frac{F_h\,\omega\,n\,A\,C_3}{F_z'\,l'\,(1+C_1)'} - \frac{F_h'\,l'\,(1+C_2)'\,W'}{F_z'\,l'\,(1+C_1)'} - \frac{F_h\,\omega\,n\,A\,C_3'}{F_z'\,l'\,(1+C_1)'}$$

and

$$u-\bar{u}^* = \frac{F_z\,l\,(1+C_1)\,(u-\bar{u}^*)}{F_z'\,l'\,(1+C_1)'} + \frac{U_n}{F_z'\,l'\,(1+C_1)'}$$

$$\frac{\left[F_z\, l\, (1+C_1)\,(v-\bar{v}^{\,*})+V_n+F_h\, l\, (1+C_2)\, W\right]\sin\theta}{F_z'\, l'\, (1+C_1)'}.$$

By normalizing by F_z' and the other factors, it is clearer why the method performance degrades near the equator. Examine first the east velocity component. In general, U_n has a white spectrum with an amplitude of about 50 nV/$\sqrt{Hz}$, which for the 0.7 Hz bandwidth typical of the normal 10 rotation average is 40 nV, or about 1 cm s^{-1} at mid-latitudes where F_z is 0.4×10^{-4} T. During this experiment the noise measured by the XCP was determined *in situ* using the shorted electrode probes (Figure 9). When the electrodes are shorted, the probe is no longer measuring water velocity. Thus, the equation for the east component reduces to

$$u-\bar{u}^{\,*}=\frac{U_n}{F_z'\, l'\, (1+C_1)'}$$

which, at 3°N, translates to a 1.2 cm s^{-1} noise contribution. The increase from the mid-latitude value is caused by the vanishing F_z'. Based on this noise level we can then model the increase in noise one would expect as one nears the magnetic equator (Figure 11); i.e.,

$$\text{rms difference}=\frac{1.2\ \text{cm s}^{-1}}{(1+C_1)\, l\, F_z}.$$

The dashed line predicts a value of 10 cm s^{-1} at 6°30'S, 1.5° from the magnetic equator. From the XCP/TOPS comparison data along 95°W and along the geographic equator, the east component agrees very well with the model, reaching a noise level of 10 cm s^{-1} between 6 and 7°S. However, the north component is more variable, degrading to 10 cm s^{-1} between 4 and 5°S, but dropping back to 6 cm s^{-1} at 6°S and finally degrading substantially south of 6°S. There is an anomalous point at 1°S, where the north rms difference reached 24 cm s^{-1}. We believe this was caused by some sort of instrument malfunction. The north velocity component may break down farther away from the magnetic equator owing to terms in the north equation that are not in the east equation. Errors in north may arise from differences between the assumed fall rate W' and the actual fall rate W. By 6°S, where F_z/F_h = 0.07, the fall rate term in the north velocity

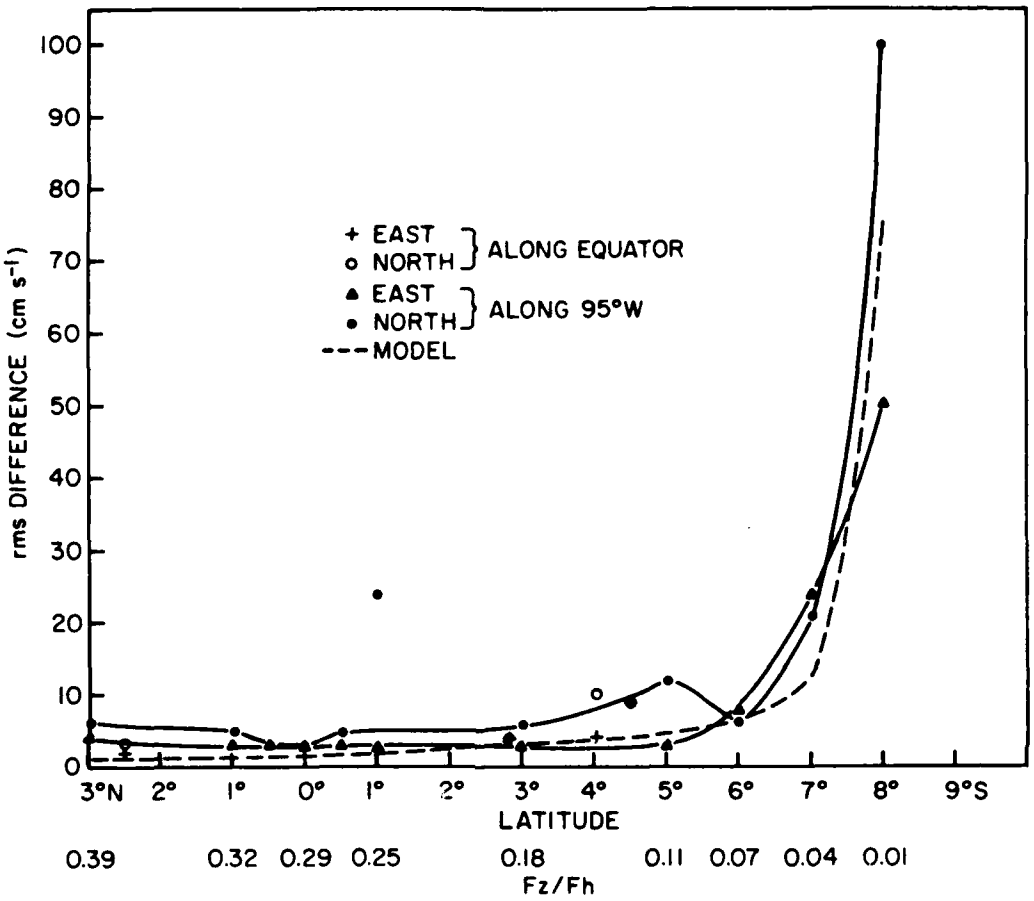

Figure 11. The rms differences between XCP and TOPS. The dashed line is the model prediction. The values of F_z/F_h for the drops in the 95°W section are shown below the corresponding latitude.

equation has a magnitude of 3000 cm s^{-1} with W equal to 450 cm s^{-1}. An error of 1% in W will result in an equivalent error in the north component of 30 cm s^{-1}. At mid-latitudes the same error is about 1 cm s^{-1}.

It is interesting to look at the relationship between latitude, Θ, and the ratio F_z/F_h. The main geomagnetic field of the earth is approximately that of a magnetic dipole aligned along the axis of rotation with components

$$F_h = \frac{M \cos\Theta}{r^3}$$

$$F_z = \frac{-2 M \sin\Theta}{r^3},$$

where

M = 8×10^{15} T m^3,
Θ = latitude (positive to the north), and
r = geocentric radius,

so that

$$\frac{F_z}{F_h} = -2 \tan\Theta,$$

which for small Θ (low latitudes) reduces to

$$\frac{F_z}{F_h} = -2\,\Theta.$$

This shows that for a change in latitude there will be a corresponding factor of two increase in F_z/F_h. This increase in F_z/F_h will subsequently lead to better XCP performance.

Another source of error may arise from the determinations of F_z and F_h. Full knowledge about the true magnetic field components at the profile sites is not available. F_z and F_h are not determined *in situ*, but rather are calculated using a spherical polynomial model based on date and time. To illustrate the uncertainty in determining F_z and F_h, two different models were used to determine the position of the magnetic equator. The results differed by approximately 30 nautical miles. The major differences between the two models, USWC75 (which we traditionally use) and IGRF, are in the Gaussian coefficients and the rate of change of the coefficients.

Another source of error affecting both velocity components is vessel contamination of the near surface currents. This was mentioned in the discussion of the nearly simul-

taneous XCP drops. It is also noticeable in the XCP/TOPS comparisons. There is occasional interference caused by electric and magnetic disturbance of the *Discoverer.* Some XCP drops show strong upper ocean shears not seen with TOPS. For example, see Figure 6b,c,g,i. The source of the structure is thought to be vessel-produced electric fields. Normally, these fields are small, being a few centimeters per second in mid-latitudes. Scaled by the ratio of horizontal to vertical magnetic field components, the electric currents due to hull corrosion or cathodic protection will produce signals equivalent to very large horizontal velocities, just as in the case of the fall speed error. Probe-to-vessel separations greater than 200 m are needed in the future in this area.

Some profiles indicate that the probe failed over some depth intervals. Figures 6g and 6i show peculiar deep structures that have been seen before at much reduced magnitudes at mid-latitudes. That these structures are in the north component is typical of electronic difficulties, such as amplifier gain.

Other sources of error arise from contributions in the theory of motional induction that are neglected in the interpretation of XCP profiles. For example, the neglected terms are of order $F_h H / F_z L$, where H and L are the vertical and horizontal length scales of the flow under study. The magnetic field ratio is about 40 in the current example, while H/L is generally 10^{-2} to 10^{-3}. Hence, this error is of order 10% or smaller of the horizontal flow, not very large compared with the fall rate error.

Is the operational limit of 1.5° suggested by Figure 11 due entirely to the vanishing of the vertical component of the earth's magnetic field, or are there instrument characteristics peculiar to the Mod 6 XCP that restrict using XCPs closer to the magnetic equator? To answer this question we can look at some data from another equatorial experiment, Tropic Heat (Figure 12), which was conducted in a geomagnetic area similar to that of the EPOCS work. The Tropic Heat data were obtained in November-December 1984 with Mod 7 XCPs. The Mod 7 XCPs use an RF link to the shipboard processing system. Tropic Heat data are available along a section with the same F_z/F_h ratios as the EPOCS 95°W data. Plotted over each other in Figure 13a are the east velocity components at similar F_z/F_h ratios. The noise increases as F_z/F_h decreases similarly for EPOCS and Tropic Heat. The degradation becomes significant between 0.04 and 0.07 F_z/F_h. A comparison of the north components yields the same pattern (Figure 13b). Thus, the limiting ratio for both these experiments, using different XCP Mods, appears to be between 0.04 and 0.07 F_z/F_h. A value of 0.05 F_z/F_h corresponds to 1.5° of latitude separation from the magnetic equator.

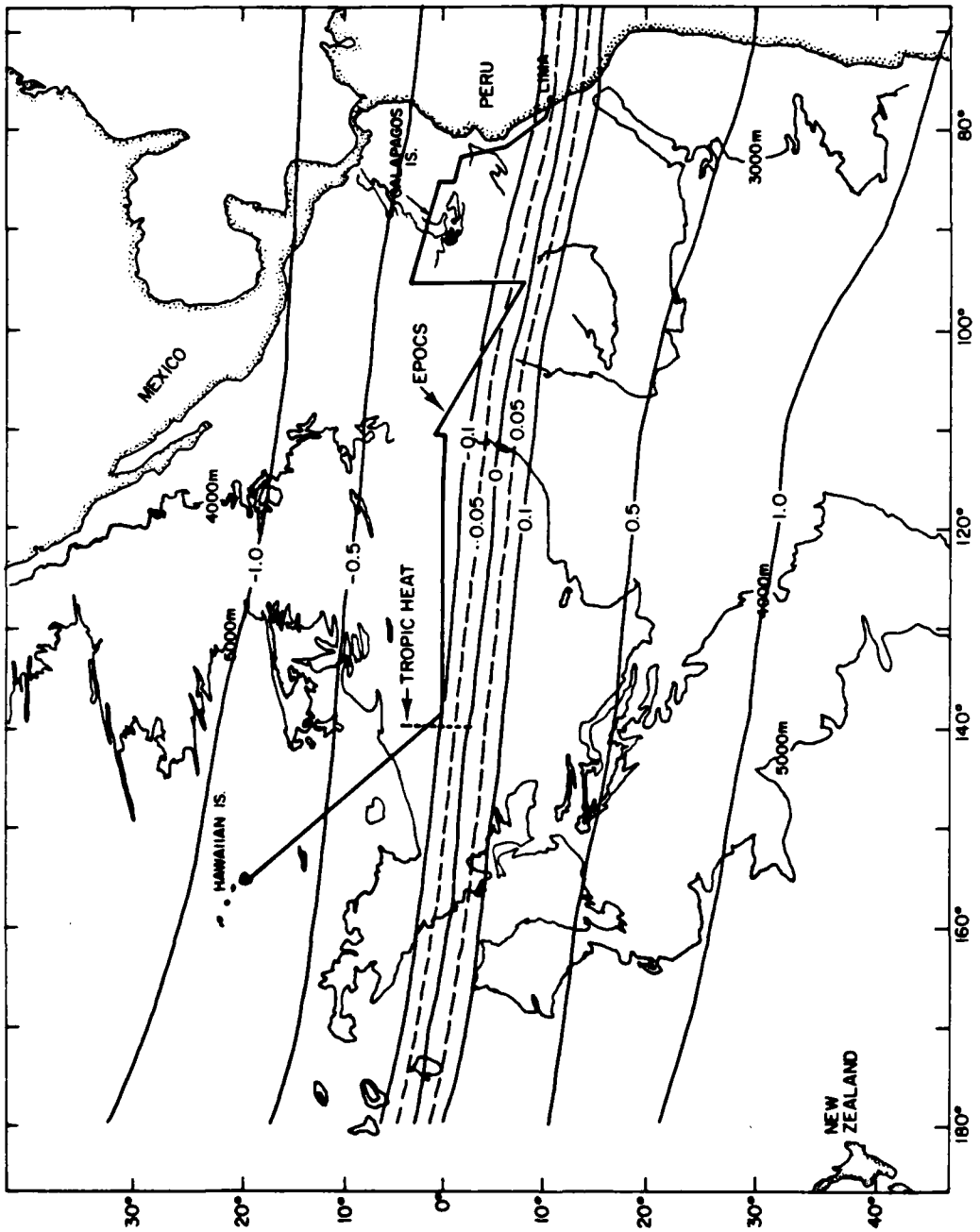

Figure 12. Equatorial area chart showing the EPOCS cruise track (solid line) and experimental site for Tropic Heat (dashed vertical line). Also shown are contours of F_z/F_h.

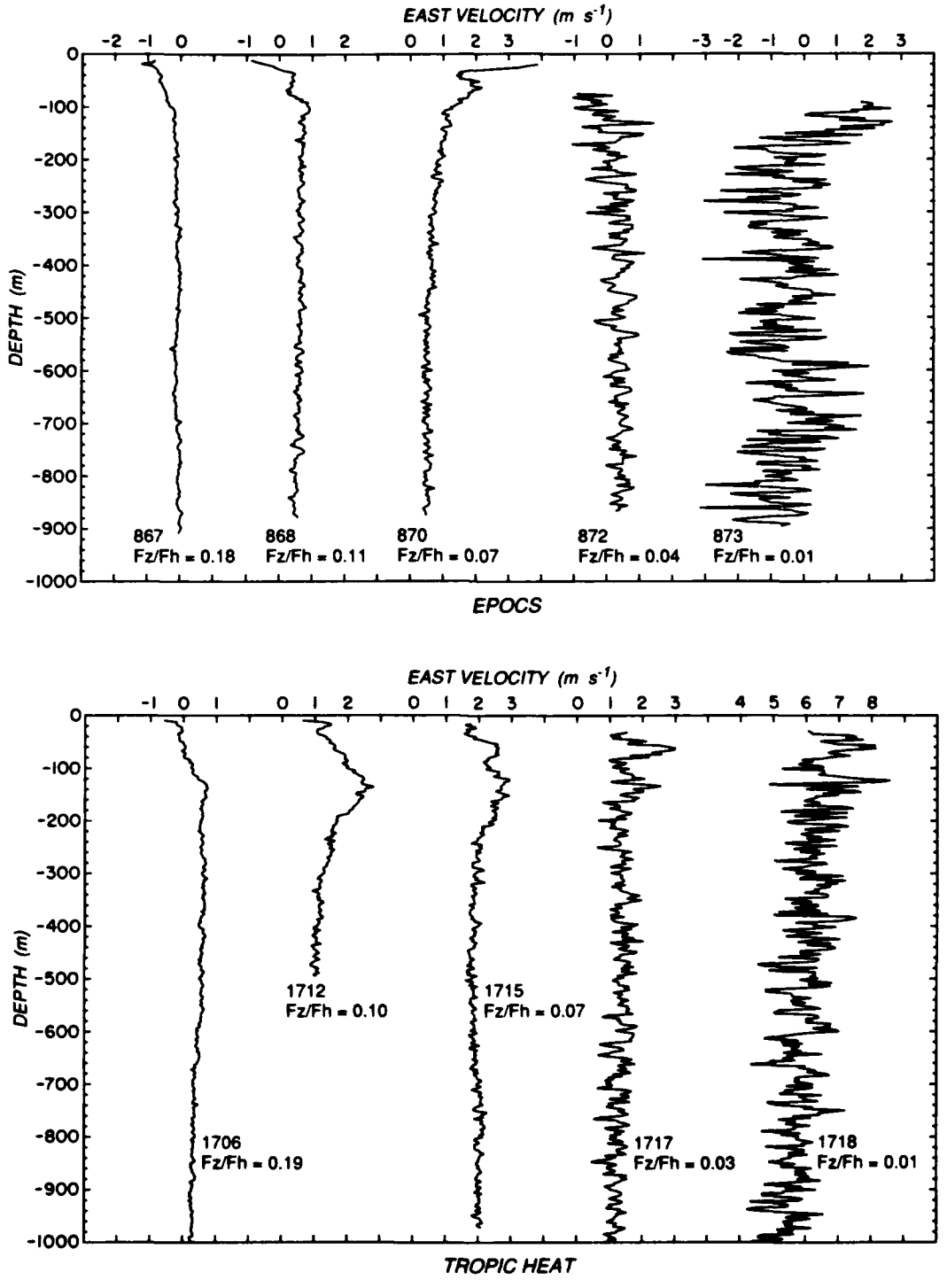

Figure 13a. Velocity comparisons at similar F_z/F_h ratios.

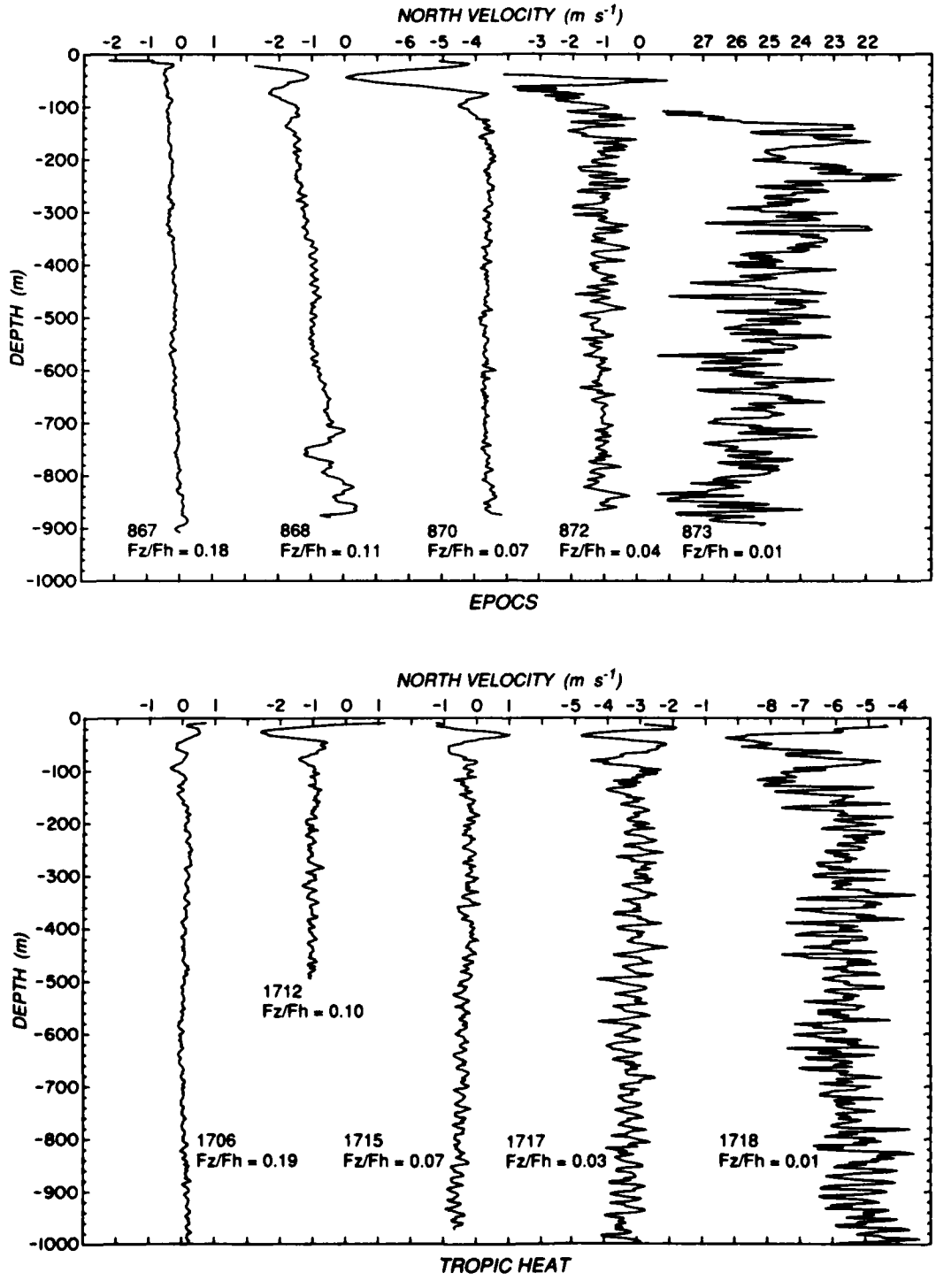

Figure 13b. Velocity comparisons at similar F_z/F_h ratios.

12. SUMMARY

The XCP performs well to within 1-2° of the magnetic equator, for the east component of velocity, corresponding to $F_z/F_h \approx 0.05$. For $F_z/F_h < 0.05$, all comparisons reveal strong differences and much variability. The difficulties encountered with near-equatorial profiling with electromagnetic profilers arise mainly from inaccurate compensation of the fall-induced signals, electronic noise, vessel interference and phase angle differences. Small changes in amplifier gain or in other characteristics of the probe and electronics may also have enhanced effects when F_z is small. The smallness of the desired signals, the first terms of the expressions on pages 32 and 33, is a limiting factor but not the most critical one. Note that it is only the vertical variations of W from the assumed values that are important. That is, since the XCP profiles, even in the best of circumstances, are relative to a depth independent offset, it is not the absolute error in W that is relevant; rather, it is the vertical fluctuation that matters. Also, the east component is not affected by the fall rate problem, except that it is always more difficult to extract the east component when the north becomes significantly larger. Electronic noise can be improved and vessel interference eliminated.

XCPs can be used in equatorial regions, but the performance will be degraded. The limiting ratio of F_z/F_h is 0.05. Thus, one should expect errors of 10 cm s^{-1} at 1.5° or so from the magnetic equator. A special chart (Figure 14) showing the ratios of vertical to horizontal magnetic field components has been made. If one stays outside the 0.05 contour, there should be little trouble. It should be pointed out that GEK measurements have similar restrictions. During some GEK work in the Indian ocean the operational limit was between 1 and 1.5° from the magnetic equator (Martin *et al.*, 1965).

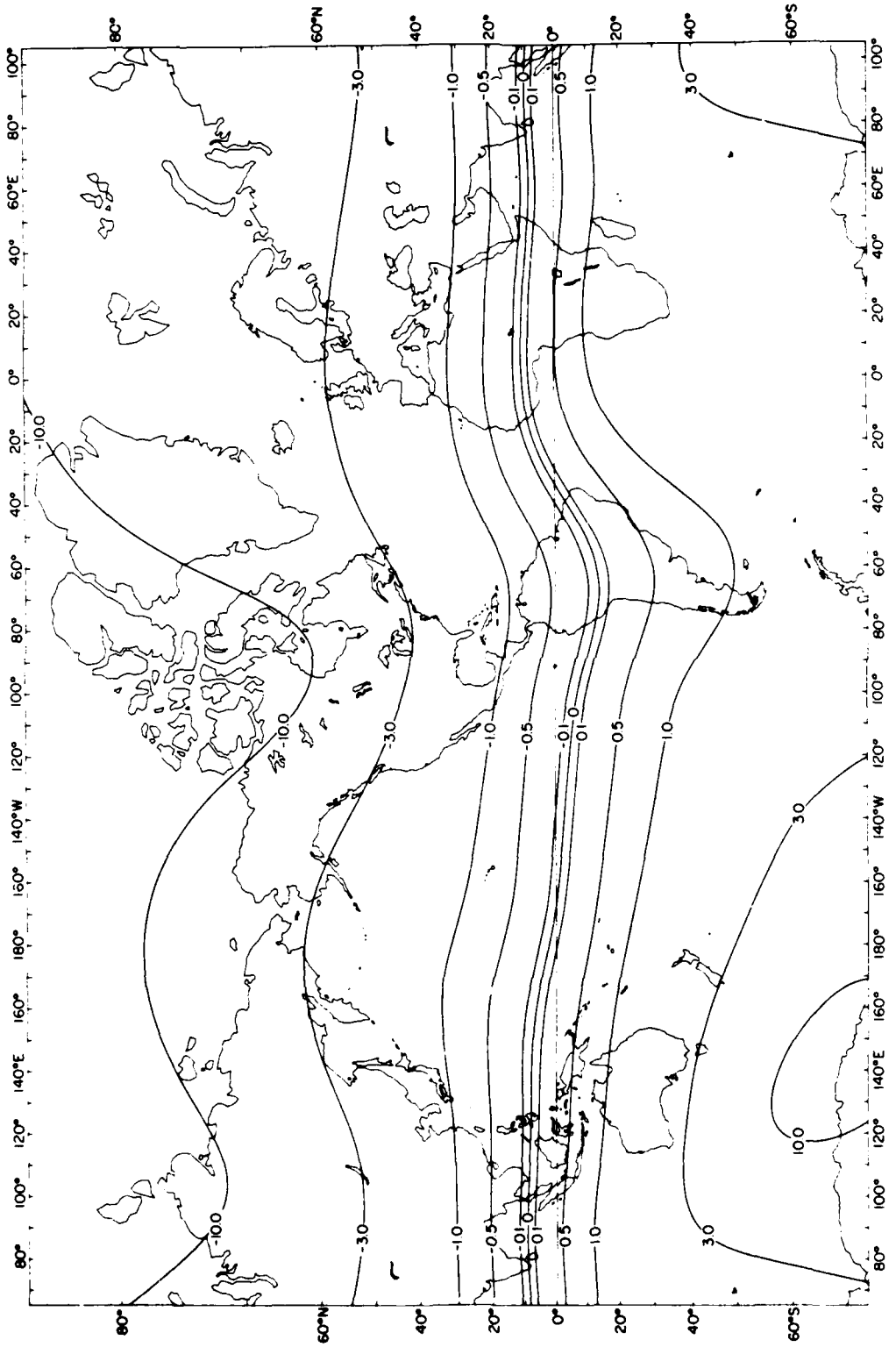

Figure 14. Contour chart of F_z/F_h.

13. ACKNOWLEDGMENTS

We thank Dr. Stan Hayes of NOAA/PMEL for making the TOPS data available for this report. Mr. Hugh Milburn, chief scientist for the EPOCS cruise, and Ms. Linda Mangum facilitated the XCP deployments. We are also grateful to Dr. Michael Gregg and Dr. Hartmut Peters for providing the Tropic Heat XCP data.

This work was supported by the Naval Ocean Research and Development Activity, Ocean Measurements Program (contract N000-14-82-C-0038).

14. REFERENCES

Drever, R.G., and T.B. Sanford, 1980, "An Expendable Temperature and Velocity Profiler (XTVP)," *Near Surface Ocean Experimental Technology Workshop Proceedings*, Naval Ocean Research and Development Activity, NSTL Station, MS, pp. 163-173.

Hayes, S.P., H.B. Milburn and E.F. Ford, 1984, "TOPS: a Free-Fall Velocity and CTD Profiler," *Journal of Atmospheric and Oceanic Technology*, 1(3), 220-236.

Martin, J., P. Guibout, M. Crepon and J.C. Lizeray, 1965, "Circulation Superficielle dans L'Ocean Indien," *Cahiers Oceanographiques*, XVII, supplement 3, pp. 221-241.

Sanford, T.B., 1982, "Velocity Profiling: Some Expectations and Assurances," *Proc. IEEE Second Working Conf. on Current Measurement*, M. Dursi and W. Woodward, eds. (IEEE, New York), pp. 101-112.

Sanford, T.B., R.G. Drever, J.H. Dunlap, and E.A. D'Asaro, 1982, "Design, Operation and Performance of an Expendable Temperature and Velocity Profiler (XTVP)," APL-UW 8110, Applied Physics Laboratory, University of Washington, Seattle, WA, 164 pp.

END

12-86

DTIC